Biomedical Research and Therapy 2023, 10(8):5810-5830

Open Access Full Text Article

Original Research

Comparison of cancer stem cell enrichment between spheroids derived from single-cell and multicellular aggregate cultures

Omar Nafiis Hairuddin[1], Badrul Hisham Yahaya[2], Mohamad Johari Ibahim[1], Abhi Verakumarasivam[3], Chan Soon Choy[4], Musalmah Mazlan[1], Nurhidayah Ab. Rahim[5], Syarifah Masyitah Habib Dzulkarnain[5], Siti Farizan Mansor[2,5,*]

Use your smartphone to scan this QR code and download this article

ABSTRACT

Introduction: Cancer stem cells (CSCs) represent a distinct group of cells within cancerous tissue that possess the ability to initiate tumorigenesis and exhibit potency, self-renewal, and drug resistance. The study of CSCs often encounters challenges in obtaining these cells of interest or generating a sufficient quantity for downstream analysis. Nevertheless, it is feasible to enrich CSCs *in vitro* by subjecting them to conditions that stimulate their CSC properties, such as prolonged exposure to drugs or radiation, or by promoting their self-renewal capability through spheroid culture. Spheroids are a specific type of cell culture that organizes cells into a three-dimensional structure, closely mimicking the *in vivo* environment. These spheroids consist of a heterogeneous cell population, including CSCs or tumor-propagating cells responsible for tumor growth and maintenance. In our study, we cultured spheroids derived from single cells as well as multicellular aggregates to enrich CSCs based on their self-renewal capability and the structural organization provided by the three-dimensional context. **Methods**: Comparing the spheroid cultures with the parental adherent monolayer cells, we observed higher expression of CSC markers, pluripotent genes, and adipogenic differentiation in both multicellular spheroids (MCS) and single cell-derived spheroids (SCDS) of the two tested cell lines. **Results**: The spheroids exhibited progressive growth in size throughout the culture period. When comparing the two methods, SCDS demonstrated greater expression of surface markers and all three pluripotent genes associated with CSCs. Furthermore, when assessing drug resistance potential and the expression of the ABCG2 drug efflux gene, only 5637 SCDS displayed increased resistance to cisplatin and upregulation of ABCG2. **Conclusion**: In conclusion, both the MCS and SCDS methods effectively enriched the population of bladder CSCs in the 5637 and HT-1376 bladder cancer cell lines. However, the SCDS method demonstrated a higher upregulation of CSC markers and pluripotent gene expression compared to MCS. It is worth noting that spheroid culture and CSC enrichment are not mutually exclusive and can coexist with increased chemotherapy resistance and upregulation of ABCG2 drug efflux gene expression. Moreover, the drug efflux capability may vary depending on the specific cell line and clonal lineage. These strategies can serve as valuable models for CSC enrichment, the study of cancer cell behavior, disease modeling, and personalized chemotherapy investigations.

Key words: Bladder Cancer, Cancer Stem Cells, Cancer Stem Cells Enrichment, 3D Culture, Spheroid, Chemotherapy Resistance, Cisplatin, ABCG2

[1]*Department of Biochemistry and Molecular Medicine, Faculty of Medicine, Universiti Teknologi MARA, Malaysia*

[2]*Department of Biomedical Sciences, Advanced Medical and Dental Institute (AMDI), Sains@Bertam, Universiti Sains Malaysia, 13200 Kepala Batas Penang, Malaysia*

Correspondence

Siti Farizan Mansor, Department of Biomedical Sciences, Advanced Medical and Dental Institute (AMDI), Sains@Bertam, Universiti Sains Malaysia, 13200 Kepala Batas Penang, Malaysia

Faculty of Health Sciences, Universiti Teknologi MARA, Cawangan Pulau Pinang, Kampus Bertam, 13200 Pulau Pinang, Malaysia

Email: sitifarizan@uitm.edu.my

History

- Received: Jun 05, 2023
- Accepted: Aug 23, 2023
- Published Online: Aug 31, 2023

DOI : 10.15419/bmrat.v10i8.823

Check for updates

BioMedPress
The Open Access Publisher

INTRODUCTION

According to the Global Cancer Observatory by the World Health Organization, bladder cancer is the fifth most common cancer worldwide and the most common cancer of the urinary system [1–3]. It was the 6^{th} most common cancer in men and the 9^{th} leading cause of cancer death in men globally in 2020. Due to the very high rate of relapse (more than 50%) after treatment [4,5], the long survival rate, and the need for costly life-long routine surveillance and therapy, urothelial cell carcinoma (UCC) has the highest per-patient total cost from diagnosis to death when compared to other common cancers, such as breast, colorectal, lung and prostate cancer [6]. The recurrence of cancers, including bladder cancer, is often related to the presence of a type of cell called the cancer stem cell (CSC), due to the cell's capability to metastasize, repair its DNA damage and efflux chemotherapy drugs out of the cell [2,3,7].

CSCs are a small population of cancer cells within a tumor bulk that carries stemness state-transitioning plasticity, "potency" and "unlimited self-renewal" capability [8–10]. The concept of CSCs began with a study on acute myeloid leukemia (AML) that was published in 1994, whereby a subpopulation of AML cells obtained from a patient were able to propa-

Cite this article : Hairuddin O N, Yahaya B H, Ibahim M J, Verakumarasivam A, Choy C S, Mazlan M, Rahim N A, Dzulkarnain S M H, Mansor S F. **Comparison of cancer stem cell enrichment between spheroids derived from single-cell and multicellular aggregate cultures**. *Biomed. Res. Ther.* 2023; 10(8):5810-5830.

[3]Department of Biological Sciences, School of Medical and Life Sciences, Sunway University, Malaysia
[4]School of Liberal Arts, Science and Technology (PUScLST), Perdana University, 50490 Kuala Lumpur, Malaysia
[5]Faculty of Health Sciences, Universiti Teknologi MARA, Cawangan Pulau Pinang, Kampus Bertam, 13200 Pulau Pinang, Malaysia

gate tumorigenesis in severe combined immunodeficient (SCID) mice after transplantation [11]. This finding drives a domino effect on the research revolving around CSCs, as later in 2003, the discovery of cancer stem cells in solid tumors, namely, breast cancer and brain cancer, was also published [12,13]. In addition, CSCs were discovered in various other cancers, such as melanoma [14], osteosarcoma [15], prostate cancer [16], ovarian cancer [17], gastric cancer [18], lung cancer [19–21], and bladder cancer [2,3,5,7].

However, research on CSCs is often restricted by the scarcity of the desired sample, as CSCs make up only a very small population of a tumor bulk [22,23] due to the feedback mechanism of self-renewal and stochastic differentiation to maintain homeostasis of an organ, or in this case, a malignant tumor, to ensure a feasible amount of functional progeny cells [8]. Because of this, some researchers aim to enrich the CSC population by various means and methods, such as isolation of CSC-related cell surface markers [18,21,24], side population (SP) cells [25,26], chemotherapy- and radiotherapy-resistant cells [22,27–30] and spheroid cultivation [10,31,32]. While some researchers opt for single-cell analysis for the study of CSCs in various cancers, including bladder cancer [5,33,34], this method is not extensively accessible and is costly.

Isolation and enrichment of CSCs through the spheroid culture method is an effective approach to studying CSCs in solid tumors because spheroid culture provides 3D organization and cell-to-cell interactions that mimic the *in vivo* tumor structure [35–38]. The formation of a 3D organization of cells in spheroids can be achieved through various methods depending on the aim of research or specimen origin. Cell-derived tumorspheres can be established through two approaches: multicellular tumor spheroids (MCTSs) and single-cell-derived tumor spheroids (SCDSs). MCTS is generated by culturing cells as multicellular aggregates, whereas SCDS is cultured as isolated single cells. Both methods can be performed with or without a scaffold, which provides structure and support that mimics the extracellular membrane *in vivo* [36,37].

The application of 3D spheroid culture as a means for drug sensitivity testing for cancer has also been widely used, as the organization of cells in a 3D cluster allows for a better model in drug sensitivity testing and drug response analysis when compared with 2D monolayer culture. As an organization of cells in a 3D structure provides a niche to support the activation of EMT and the pluripotent pathway, which increases the number of CSCs [39], this could also indirectly increase the drug resistance capability of the spheroid, as CSCs are known to be resilient to chemotherapy drugs by the activation of several pathways, such as the ABCG2 drug efflux pathway [40].

In this study, spheroids were grown from either multicellular aggregates or single cells to mimic the cell–cell organization of *in vivo* tumors and the self-renewal capability of CSCs, to provide methods for CSC enrichment and to test whether the culture of cells in a 3D organization and the enrichment of CSCs will result in a model system that is suitable for *in vitro* analysis of drug resistance *in* bladder cancer (**Figure 1**).

METHODS

Cell lines and culture media

The bladder cancer cell lines 5637 and HT-1376 were purchased from American Type Culture Collection (ATCC, Rockville, MD, USA). The parental adherent monolayer 5637 and HT-1376 cell lines were maintained in RPMI 1640 complete media consisting of Roswell Park Memorial Institute (RPMI) 1640 basal media (Corning, USA) supplemented with 25 mM HEPES (Gibco, Thermo Fisher Scientific, USA), 10% fetal bovine serum (FBS) (Gibco, Thermo Fisher Scientific, USA) and 1% penicillin–streptomycin in an incubator with 5% CO_2 at 37°C. Spheroids were cultured in RPMI 1640 spheroid media consisting of RPMI 1640 basal medium supplemented with 1x B27 supplement (Gibco, Thermo Fisher Scientific, USA), 0.4% FBS (Gibco, Thermo Fisher Scientific, USA), 20 ng/ml basic fibroblast growth factor (bFGF) (R&D Systems, USA), 20 ng/ml epidermal growth factor (EGF) (R&D Systems, USA), 4 μg/ml insulin (Gibco, Thermo Fisher Scientific, USA) and 1% penicillin–streptomycin (Corning, USA).

Multicellular Spheroid (MCS) Culture

5637 and HT-1376 cells were cultured in RPMI complete media as monolayers until 80% confluence. Cells were then dissociated by adding 0.25% trypsin-EDTA (Gibco, Thermo Fisher Scientific, USA) for 5 minutes at 37°C to obtain a single-cell suspension. A suspension of 200,000 cells/ml was prepared using RPMI spheroid media in a 50 ml tube and transferred to a trough. Twenty-five microliters of the suspension was pipetted using a multichannel pipette onto a sterile petri dish as droplets containing 5000 cells. The petri dish was then inverted upside down and cultured for 2 days to form MCSs. The MCSs were transferred to 24-well ultralow attachment (ULA) plates containing 500 μL of RPMI 1640 spheroid media and cultured for 8 days with media replenishment every 3 days. The MCS morphology and diameter were observed and measured at 4 different timepoints (day

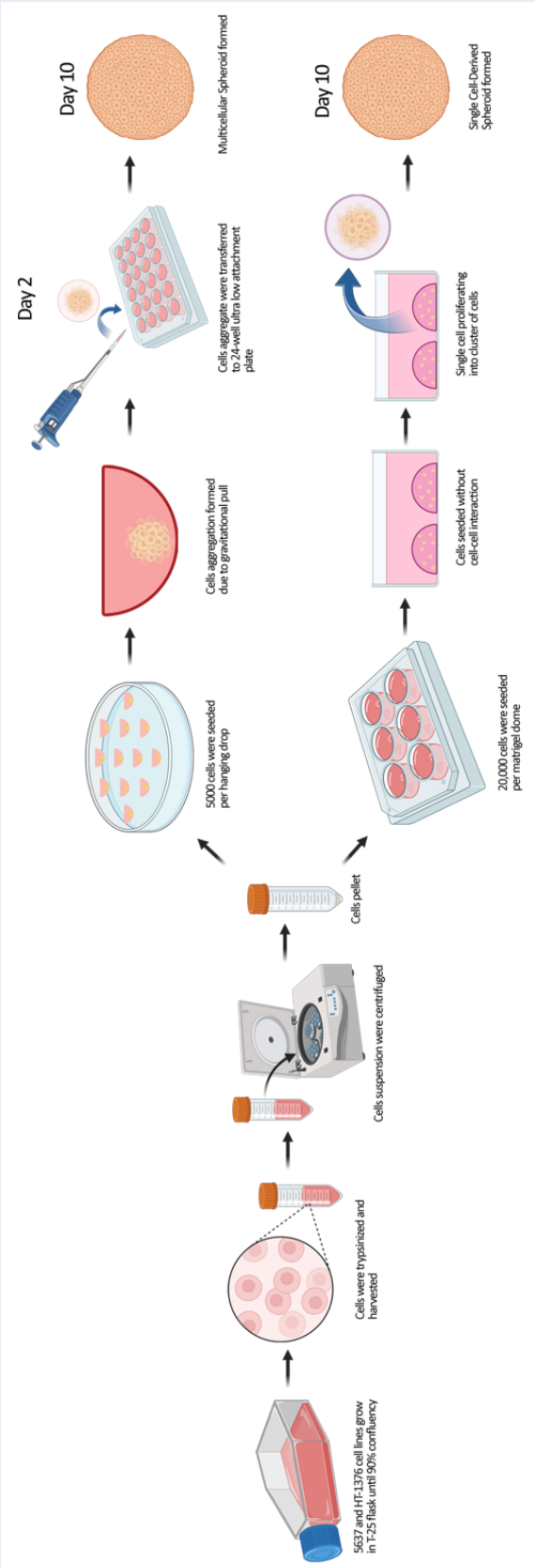

Figure 1: **Illustration of the overview methodology for the Multicellular Spheroid (MCS) and Single Cell-Derived Spheroid (SCDS) development from 5637 and HT-1376 Bladder Cancer Cell Lines.** Image created using biorender.com.

2, day 5, day 7 and day 10) using an inverted phase contrast microscope (Olympus IX51) and were then harvested after day 10 of culture, which consisted of 2 days in the hanging drop and 8 days in the ULA plate. MCSs were collected in a 15 ml tube and centrifuged at 1500 rpm for 5 minutes. The supernatant was decanted, and the cell pellet containing MCSs was gently mixed with 0.25% trypsin-EDTA and shaken at 300 rpm at 37°C to dissociate the MCSs and obtain a single-cell suspension to be used in downstream experiments.

Single Cell-Derived Spheroid (SCDS) Culture

5637 and HT-1376 cells were cultured in RPMI complete media as a monolayer until 80% confluence. Cells were then dissociated by adding 0.25% trypsin-EDTA (Gibco, Thermo Fisher Scientific, USA) for 5 minutes at 37°C to obtain a single-cell suspension. At 4°C (on ice), 20,000 cells from the single-cell suspension were added to a 1.5 ml Eppendorf tube. Additional media was added if required until the volume reached 7.5 μl. The cells were mixed with 7.5 μl of Matrigel^{TM} (Corning, USA) to establish a 15 μl cell:Matrigel mixture at a 50:50 ratio containing 20,000 cells. The cell:Matrigel mixture was pipetted onto a 24-well plate as a dome-shaped droplet and kept in a 37°C incubator for 30 minutes for the Matrigel^{TM} to solidify. Then, 500 μl of spheroid media was added and cultured for 10 days with media replenishment every 3 days. The SCDS morphology and diameter were observed and measured at 4 different timepoints (day 2, day 5, day 7 and day 10) using an inverted phase contrast microscope (Olympus IX51) and harvested after day 10 of culture. SCDS was collected in a 15 ml tube and centrifuged at 1500 rpm for 5 minutes. The supernatant was decanted, and the cell pellet containing MCSs was gently mixed with 0.25% trypsin-EDTA and shaken at 300 rpm at 37°C to dissociate the MCSs and obtain a single-cell suspension to be used in downstream experiments.

Bladder cancer stem cell-related surface marker analysis by flow cytometry

The stem-like characteristics of the MCSs and SCDSs were determined by flow cytometry analysis of CD24, CD44 and CD133. A total of 2 x 10^5 cells harvested from MCSs and SCDSs were added to 15 ml tubes labeled with CD24/CD44, CD44/CD133, CD24/CD133, APC, FITC, PE and unstained. Cells were washed one time with 1x sterile PBS and centrifuged at 1500 rpm for 5 minutes, and the supernatant was decanted. Cells were then resuspended in 200 μl FACS staining buffer and stained with 2 μl of anti-CD24-PE antibody (BD Biosciences, USA), anti-CD44-FITC antibody (BD Biosciences, USA) and anti-CD133-APC (Miltenyi Biotec, USA) antibody according to the tube label for 40 minutes in the dark at 4°C. Cells were then washed one time with 1x sterile PBS, resuspended in 200 μl FACS staining buffer and further analyzed using a flow cytometer. The expression of CD24, CD44 and CD133 in MCS and SCDS cells was compared to that in parental cells.

Quantitative Real-Time PCR (qRT–PCR) analysis of Pluripotent Transcriptional Factor of *SOX2, NANOG* and *POU5F1* and *ABCG2* Drug Efflux gene expression

Total RNA was extracted from MCS and SCDS using a Nucleospin^{TM} RNA plus extraction kit (Macherey-Nagel, Düren, Germany) according to the manufacturer's recommendation, and the RNA concentration and purity were measured using Nanodrop and converted to cDNA using a Tetro^{TM} cDNA Synthesis Kit (Meridian Life Science Inc., USA) according to the manufacturer's recommendation. Real-time qPCR was performed to determine the expression of pluripotency genes (*SOX2, NANOG, POU5F1*) and a drug efflux gene (ABCG2) in 100 ng of cDNA from MCS and SCDS cells using a SensiFAST^{TM} Probe Hi-ROX Kit and analyzed by an Applied Biosystems 7500 fast instrument (Meridian Life Science Inc., USA). Fluorescent-probed primers were obtained from Applied Biosystems (CA, USA): GAPDH (control) Hs02758991_g1, SOX2 Hs01053049_s1, NANOG Hs04399610_g1, POU5F1 Hs00999632_g1 and ABCG2 Hs01053790_m1. Ten microliters of 2x SensiFAST Probe Hi-ROX Mix, 1 μl of fluorescent-probed primers, 100 ng of cDNA, and H_2O were added until the final reaction mix was 20 μl. Gene amplification was performed as follows: 95°C for 2 minutes (1 cycle), 95°C for 10 seconds and 60°C for 50 seconds (40 cycles). The mRNA values of SOX2, NANOG, POU5F1 and ABCG2 were normalized to the GAPDH (control) values in each sample by subtracting the mean Ct (cycle threshold) values of the control sample from the Ct values of the genes of interest (SOX2, NANOG, POU5F1, ABCG2). The expression of *SOX2, NANOG, POU5F1* and *ABCG2* in MCS and SCDS cells was compared to that in parental cells.

Adipogenic and osteogenic lineage differentiation *in vitro* analysis

The MCS and SCDS of both cell lines were induced to differentiate into adipogenic and osteogenic lineages

using differentiation media (Stempro™, Thermo Fisher Scientific, USA). Briefly, cells harvested from MCS and SCDS were cultured in a 24-well plate in RPMI spheroid media until 80-90% confluence. The RPMI 1640 complete culture medium in three of the wells was replaced with differentiation media (Stempro™, Thermo Fisher Scientific, USA) to induce differentiation. Another three wells were maintained in RPMI 1640 complete culture medium as a control and cultured for 14 days (adipogenesis) and 21 days (osteogenesis), and the medium was replenished every 3 days. At the end of culture, cells were washed with 1x sterile PBS, fixed with 10% neutral buffered formalin and stained with Oil Red O staining for adipogenesis to observe the formation of lipid vesicles or Alizarin Red S staining for osteogenesis to detect calcium deposition. Cells were then washed with distilled water to remove any excess stain, added to 500 μl of 1x sterile PBS and observed under an inverted phase contrast microscope (Olympus IX51).

Adipogenesis and osteogenesis differentiation imaging analysis

After staining with the respective staining method, culture images of adipogenic differentiation and osteogenic differentiation of 5637 and HT-1376 parental, MCS, SCDS and UC-MSC (positive control for mesodermal lineage differentiation) were captured using an inverted phase contrast microscope (Olympus IX51). The percentage (%) of adipogenic and osteogenic differentiation color intensity was analyzed using ImageJ color threshold by using the formula: (color threshold of the fat droplet in Oil Red-O stain or calcium deposition in Alizarin Red stain/color threshold of whole image) x 100%.

Cell viability assay and cisplatin inhibitory concentration 50 (IC_{50})

Parental monolayer adherent bladder cancer cells of both the 5637 and HT-1376 cell lines were seeded in 96-well plates at a seeding density of 5000 cells/well in RPMI-1640 complete media with a final volume of 100 μl per well. Cells were incubated for 48 hours in a humidified 5% CO_2 incubator at 37°C. After 48 hours, the media were replaced with media containing a gradually increasing concentration of cisplatin, and the cells were further incubated for 48 and 72 hours for treatment. After treatment, 10 μl of MTT reagent was added to each well and incubated again in a humidified 5% CO_2 incubator at 37°C for 4 hours. After the incubation time, media containing MTT reagent was removed, and 100 μl DMSO was added to each well and incubated in a humidified 5% CO_2 incubator at 37°C for 10 minutes to dissolve the formazan crystal formed. Absorbance in triplicate of each well was measured using FlourOmega at 570 nm and 620 nm, using a well without treatment as a blank. The percentage of cell viability was determined for each concentration of cisplatin, and the IC_{50} concentration was determined by plotting a graph of percentage viability against drug concentration.

Spheroid chemotherapy resistance assay

After 10 days of spheroid culture, the MCSs and SCDSs were retrieved and recultured in Matrigel™ (Corning, USA) at a 50:50 ratio of media:Matrigel for cisplatin treatment. Spheroids were embedded in Matrigel™ (Corning, USA) to ensure immobilization of spheroids. Initially, spheroids were harvested from the MCS and SCDS culture methods and added to the newly prepared media:Matrigel mixture. Fifteen microliters of the media:Matrigel mixture was then pipetted on a 24-well plate to form a dome-shaped droplet, with 2 domes per well, and kept in a 37°C incubator for 30 minutes for the Matrigel™ to solidify. Then, 500 μl of spheroid media was added to the well and cultured for 2 days to ensure that spheroids were able to survive in the new environment. After 2 days of culture, the spheroid media was replenished with new spheroid media containing the IC_{50} dose of cisplatin. The IC_{50} dose of cisplatin for 5637 was 1.1 μm and 2.75 μm for HT-1376 (IC_{50} dose obtained by MTT assay of parental adherent monolayer cells of both cell lines that were treated for 48 hours with cisplatin). Spheroids were treated for 48 hours with an IC_{50} dose of cisplatin. Spheroid morphology and diameter pretreatment and posttreatment were captured and recorded.

Statistical Analysis

Statistical analysis was performed using GraphPad Prism 9 version 9.4 (GraphPad Software, California, USA). The results obtained were tested using one-way ANOVA or t-test analysis to assess the statistical significance of differences between the control group and experimental groups. Differences were considered statistically significant when $p \leq 0.05$, whereas $p \leq 0.0001$ was considered highly significant.

RESULTS

Multicellular Spheroid (MCS) and Single Cell-Derived Spheroid (SCDS) culture of 5637 and HT-1376 cells

5637 and HT-1376 cells were tested for their capability to generate and maintain a 3D spheroid structure

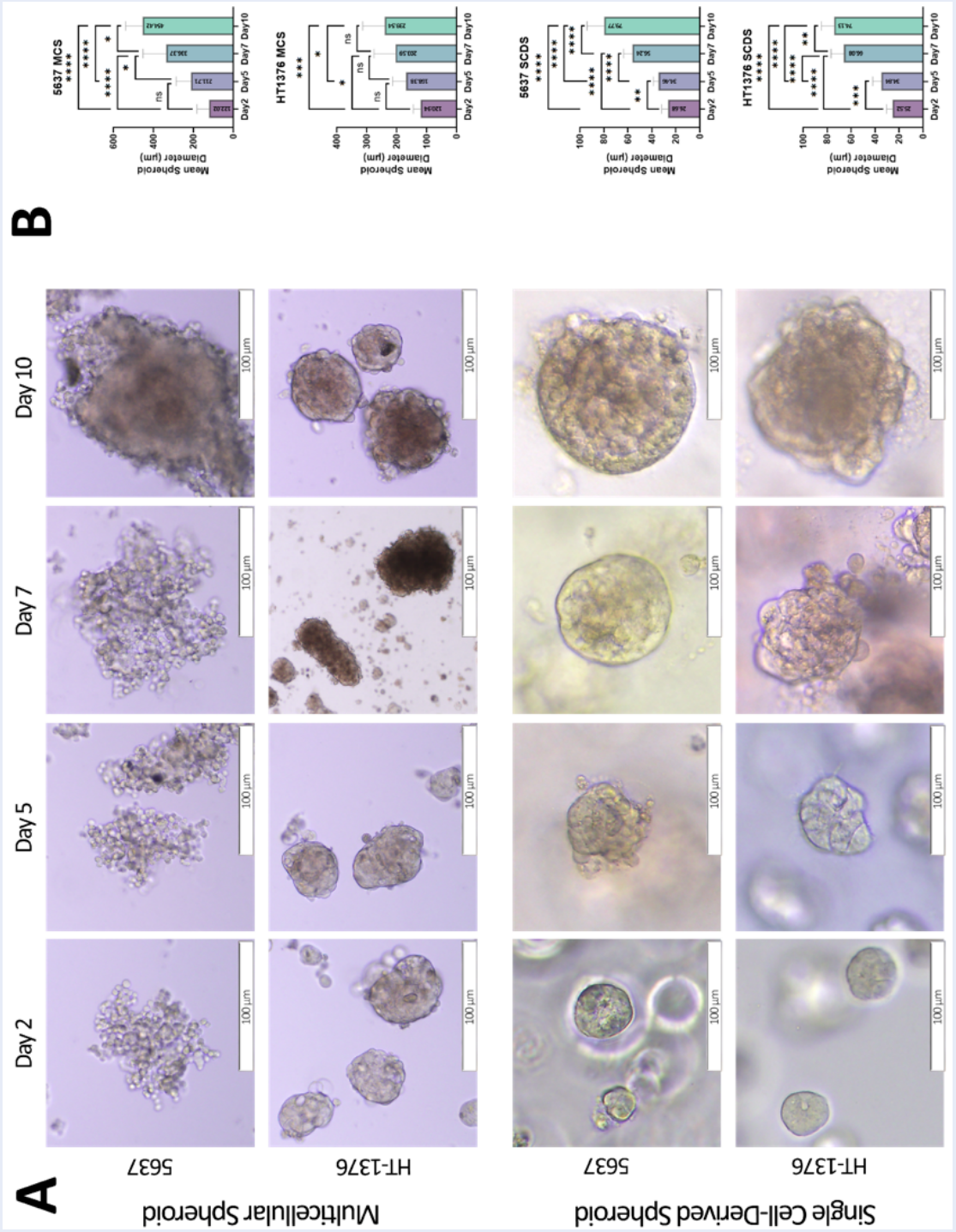

Figure 2: **MCS and SCDS of 5637 and HT-1376**. (**A**) Culture image of MCS and SCDS of 5637 and HT-1376 cells at day 2, day 5, day 7 and day 10, taken at x10 magnification. (**B**) Bar chart of mean spheroid diameter (µm) of MCS and SCDS for 5637 and HT-1376 at day 2, day 5, day 7 and day 10. The bars are represented as mean +SD (n = 10). Statistical significance was measured with the two-way ANOVA. *p < 0.05, **p < 0.005, ***p < 0.0005, ****p < 0.0001, ns = not significant. **Abbreviations**: **MCS**: Multicellular Spheroid, **SCDS**: Single Cell-Derived Spheroid

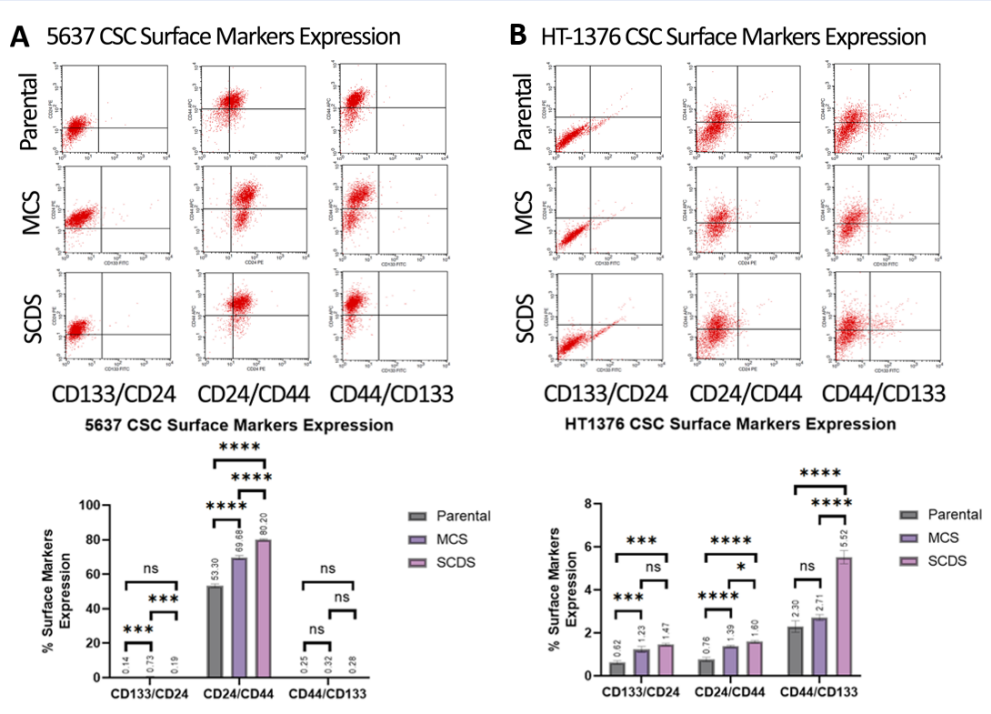

Figure 3: **Flow cytometry analysis of 5637 and HT-1376 Parental, MCS and SCDS CSC Surface Markers (CD133/CD24, CD24/CD44, CD44/CD133) expression**. (**A**) Bar chart and dot plot of 5637 Parental, MCS and SCDS CSC Surface Markers (CD133/CD24, CD24/CD44, CD44/CD133) expression. (**B**) Bar chart and dot plot of HT-1376 Parental, MCS and SCDS CSC Surface Markers (CD133/CD24, CD24/CD44, CD44/CD133) expression. The bars are represented as mean +SD (n = 3). Statistical significance was measured with the two-way ANOVA. *p < 0.05, **p < 0.005, ***p < 0.0005, ****p < 0.0001, ns = not significant. **Abbreviations**: **CSC**: Cancer stem cell, **MCS**: Multicellular Spheroid, **SCDS**: Single Cell-Derived Spheroid

using Matrigel^{TM} as a scaffold/matrix for SCDS and Ultra-Low Attachment Plate for culture without scaffold/matrix for the MCS. Both cell lines were able to form spheroids of different morphologies according to the culture method used.

According to Kenny *et al.* (2007), spheroids can be classified into four different morphological groups: round, mass, grape-like and stellate. For the 5637 cell line, in the MCS culture, the cells formed a grape-like cluster with loose aggregation and poor cell–cell adhesion, resulting in a spheroid structure that was easily dissociated but tended to aggregate with neighboring spheroids. In the SCDS culture, 5637 cells formed a round sphere with a smooth border and very robust cell–cell adhesion (**Figure 2 A**). However, for the HT-1376 cell line, in both MCS and SCDS culture, the cells formed a spheroid mass with an irregular border with strong cell–cell adhesion (**Figure 2 A**).

In terms of spheroid size, the spheroid size for MCSs (both 5637 and HT-1376) was larger than that for SCDSs (both 5637 and HT-1376) at all time points (day 2, day 5, day 7 and day 10). The initial mean spheroid diameters for the MCS were 122.02 μm (5637) and 120.94 μm (HT-1376), while the initial mean spheroid diameters for the SCDS were 26.68 μm (5637) and 25.52 μm (HT-1376) (**Figure 2B**). On day 10 of culture, the mean spheroid diameter for MCS was 454.42 μm (5637) and 239.54 μm (HT-1376), while the mean spheroid diameter for SCDS was 79.77 μm (5637) and 74.13 (HT-1376) (**Figure 2 B**). Both MCS and SCDS for 5637 and HT-1376 cells showed significant ($p < 0.001$ and $p < 0.0001$, respectively) increases in spheroid diameter when comparing the initial (day 2) to the endpoint (day 10) spheroid diameter.

CSC marker expression in the MCS and SCDS of 5637 and HT-1376 cells

The expression of CSC markers in the MCS and SCDS in 5637 and HT-1376 cells was determined using flow cytometry. Higher expression of all CSC marker combinations, CD24 and CD44, CD44 and CD133, and

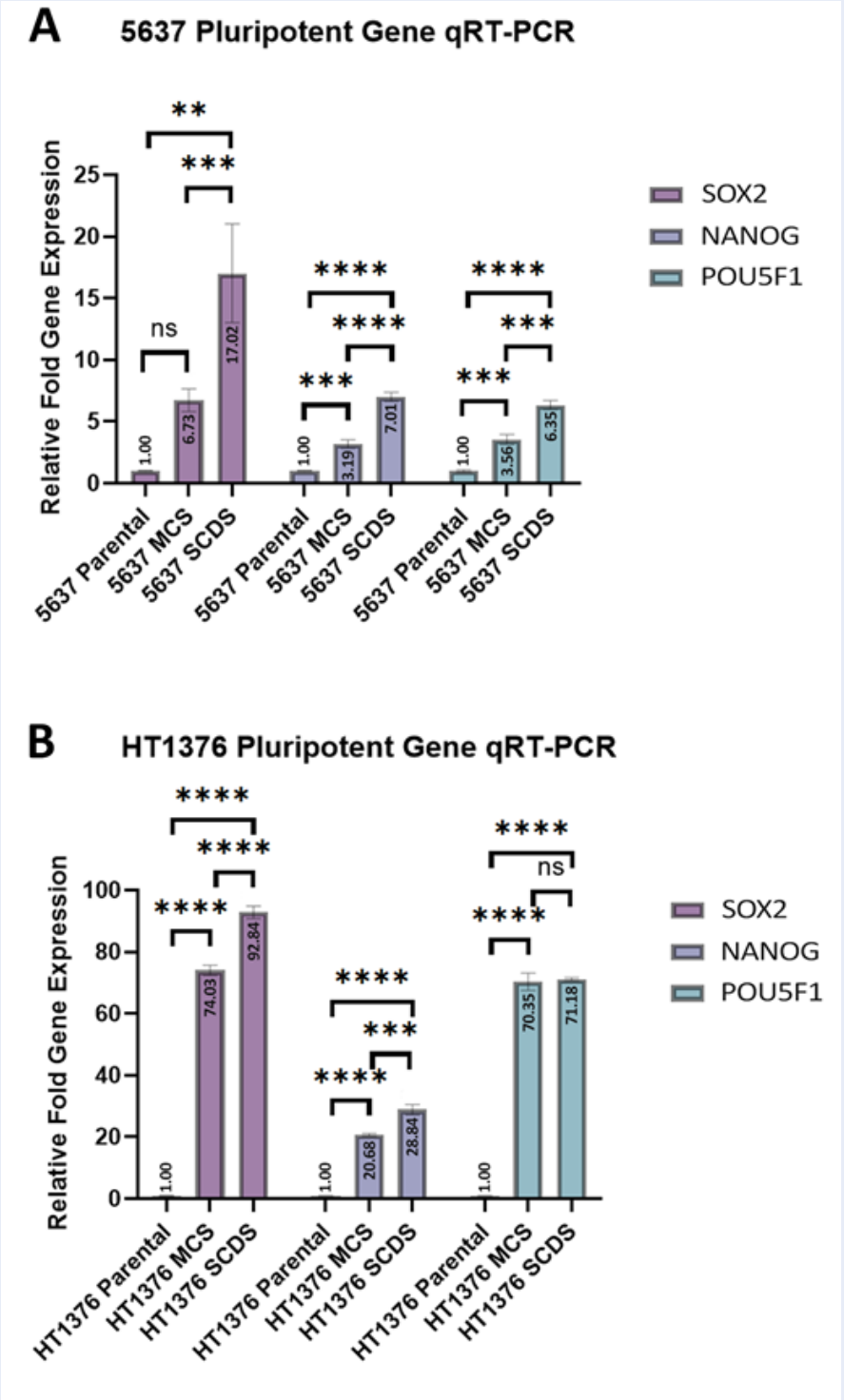

Figure 4: **qRT-PCR analysis of 5637 and HT-1376 Parental, MCS and SCDS pluripotent genes (*SOX2, NANOG, POU5F1*) expression**. (**A**) Bar chart of 5637 Parental, MCS and SCDS relative fold gene expression of pluripotent genes (*SOX2, NANOG, POU5F1*) by qRT-PCR. (**B**) Bar chart of HT-1376 Parental, MCS and SCDS relative fold gene expression of pluripotent genes (*SOX2, NANOG, POU5F1*) by qRT-PCR. The bars are represented as mean +SD (n = 3). Statistical significance was measured with the two-way ANOVA. *p < 0.05, **p < 0.005, ***p < 0.0005, ****p < 0.0001, ns = not significant. **Abbreviations**: **MCS**: Multicellular Spheroid, **SCDS**: Single Cell-Derived Spheroid

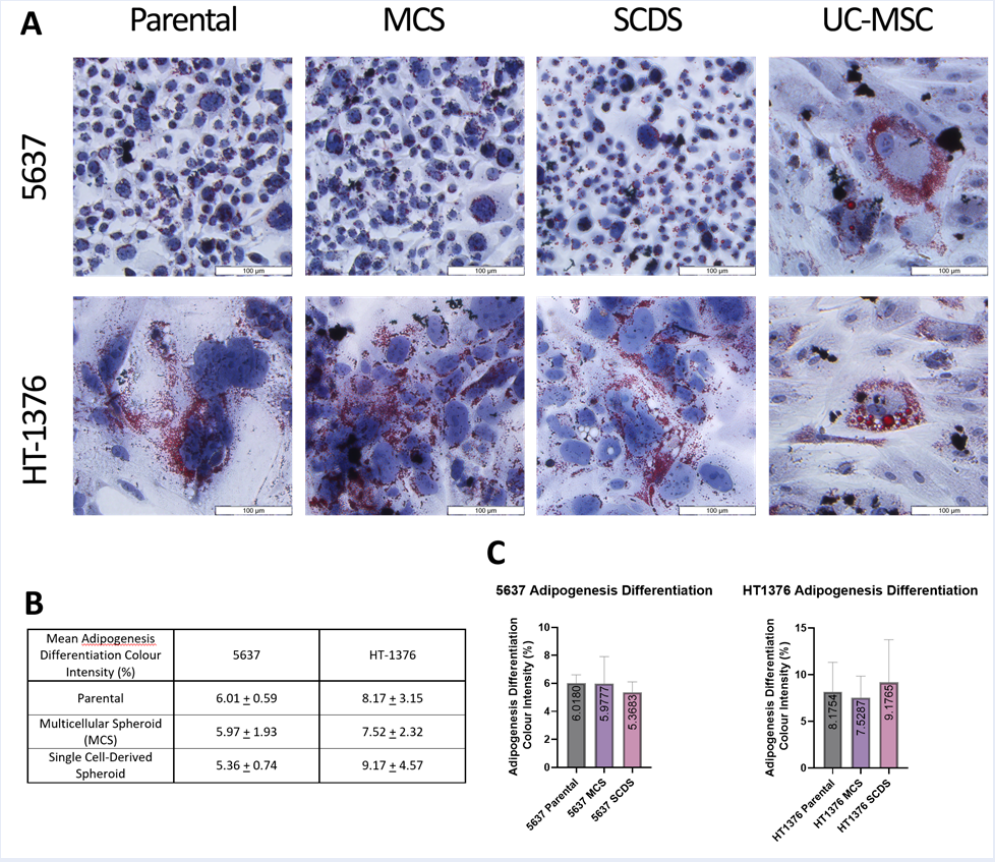

Mean Adipogenesis Differentiation Colour Intensity (%)	5637	HT-1376
Parental	6.01 ± 0.59	8.17 ± 3.15
Multicellular Spheroid (MCS)	5.97 ± 1.93	7.52 ± 2.32
Single Cell-Derived Spheroid	5.36 ± 0.74	9.17 ± 4.57

Figure 5: **Adipogenesis differentiation of parental cells of 5637 and HT-1376, MCS and SCDS of 5637 and HT-1376, and UC-MSC**. (**A**) Oil Red-O staining of parental cells of 5637 and HT-1376, MCS and SCDS of 5637 and HT-1376, and UC-MSC taken at x20 magnification. (**B**) Table showing mean adipogenesis differentiation colour intensity (%) + standard error of 5637 and HT-1376 parental, MCS and SCDS. (**C**) Bar chart showing comparison in mean adipogenesis differentiation colour intensity (%) + standard error of 5637 and HT-1376 parental, MCS and SCDS. **Abbreviations**: **IC_{50}**: Inhibitory Concentration 50%, **MCS**: Multicellular Spheroid, **UC-MSC**: Umbilical cord derived mesenchymal stem cells, **SCDS**: Single Cell-Derived Spheroid

CD133 and CD24, was found in the MCS and SCDS of 5637 and HT-1376 cells compared to parental cells. The $CD24^+CD44^+$ coexpression in the 5637 MCS was 69.67%, the $CD44^+CD133^+$ coexpression was 0.32%, and the $CD133^+CD24^+$ coexpression was 0.73%. The SCDS for 5637 cells showed 80.2% $CD24^+CD44^+$ coexpression, 0.28% $CD44^+CD133^+$ coexpression and 0.19% $CD133^+CD24^+$ coexpression (**Figure 3 A**).

The HT-1376 MCS had $CD24^+CD44^+$ coexpression of 1.38%, $CD44^+CD133^+$ coexpression of 2.71% and $CD133^+CD24^+$ coexpression of 1.23%. The SCDS for HT-1376 cells showed $CD24^+CD44^+$ coexpression of 1.59%, $CD44^+CD133^+$ coexpression of 5.52% and $CD133^+CD24^+$ coexpression of 1.46% (**Figure 3 B**).

Pluripotency gene expression in the MCS and SCDS of 5637 and HT-1376 cells

Following the increase in the coexpression of CSC-related markers when investigated by flow cytometry analysis, further investigation was performed on the RNA collected from MCSs and SCDSs of both cell lines to determine the expression of stem cell transcription factors such as SOX2, NANOG and POU5F1. Analysis was performed using the qRT–PCR method, and the relative expression of the genes in MCS and SCDS of both cell lines was compared with the expression of the genes in the parental monolayer adherent cells of each cell line. The expression of *SOX2*, *NANOG* and *POU5F1* in both the MCS and SCDS of both cell lines was upregulated at the transcriptional level (**Figure 4**).

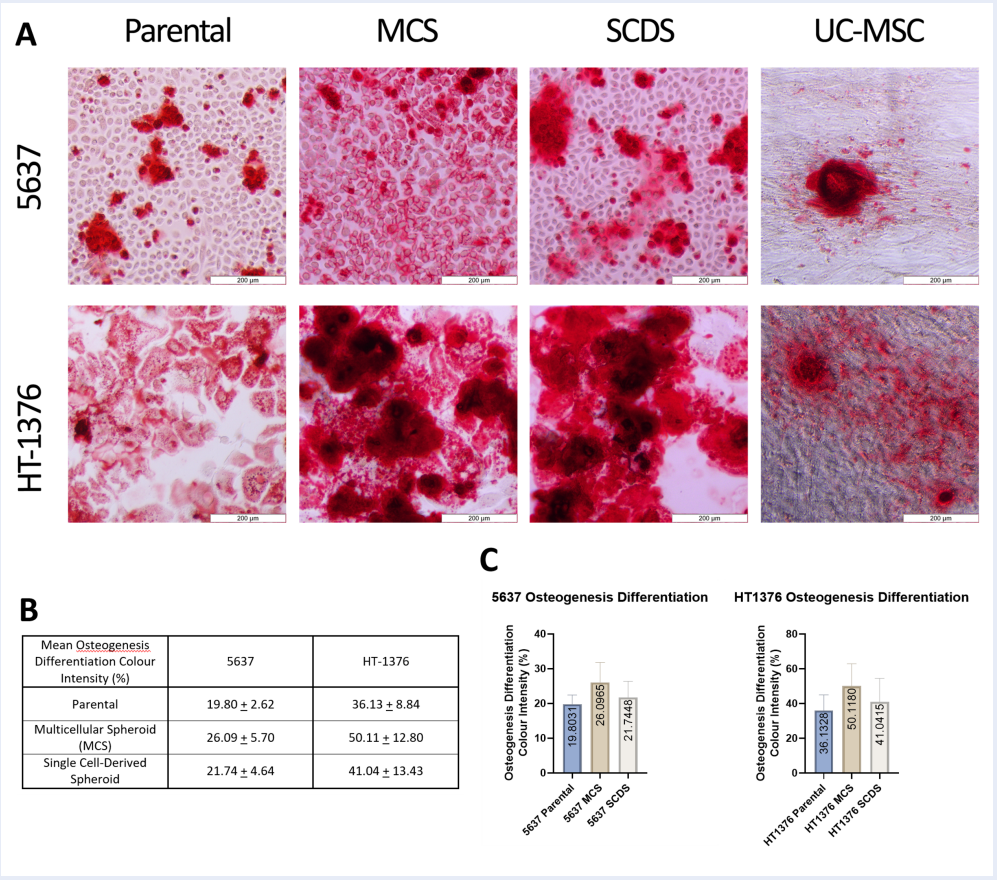

Mean Osteogenesis Differentiation Colour Intensity (%)	5637	HT-1376
Parental	19.80 ± 2.62	36.13 ± 8.84
Multicellular Spheroid (MCS)	26.09 ± 5.70	50.11 ± 12.80
Single Cell-Derived Spheroid	21.74 ± 4.64	41.04 ± 13.43

Figure 6: **Osteogenesis differentiation of parental cells of 5637 and HT-1376, MCS and SCDS of 5637 and HT-1376, and UC-MSC**. (**A**) Alizarin Red staining of parental cells of 5637 and HT-1376, MCS and SCDS of 5637 and HT-1376, and UC-MSC taken at x10 magnification. (**B**) Table showing mean osteogenesis differentiation colour intensity (%) + SD of 5637 and HT-1376 parental, MCS and SCDS. (**C**) Bar chart showing comparison in mean osteogenesis differentiation colour intensity (%) + SD of 5637 and HT-1376 parental, MCS and SCDS. **Abbreviations**: **IC_{50}**: Inhibitory Concentration 50%, **MCS**: Multicellular Spheroid, **UC-MSC**: Umbilical cord derived mesenchymal stem cells, **SCDS**: Single Cell-Derived Spheroid

Both MCS and SCDS of 5637 cells showed upregulation of the pluripotent genes *SOX2*, *NANOG* and *POU5F1* compared to parental cells. For *SOX2*, the relative fold gene expression was 6.73 in 5637 MCS cells and 17.02 in 5637 SCDS cells ($p > 0.05$ and $p < 0.01$, respectively). *NANOG* relative fold gene expression for 5637 MCS and SCDS was 3.19 and 7.01 ($p < 0.001$ and $p < 0.0001$), while for *POU5F1*, 5637 MCS and SCDS relative fold gene expression was 3.56 and 6.35 ($p < 0.001$ and $p < 0.0001$) (**Figure 4 A**).

In HT-1376 cells, both the MCS and SCDS of HT-1376 cells showed upregulation of all 3 pluripotent genes compared to parental cells. The *SOX2* relative fold gene expression was 74.03 in HT-1376 MCS cells and 92.84 in HT-1376 SCDS cells ($p < 0.0001$). *NANOG* relative fold gene expression for HT-1376 MCS and SCDS was 20.68 and 28.84 ($p < 0.0001$), while for *POU5F1*, HT-1376 MCS and SCDS relative fold gene expression were 70.35 and 71.18 ($p < 0.0001$) (**Figure 4 B**).

Osteogenic and adipogenic differentiation capabilities of the MCS and SCDS of 5637 and HT-1376 cells

Osteogenic and adipogenic differentiation culture was performed on the MCS and SCDS of 5637 and HT-1376 cells to investigate the lineage differentiation capability of cancer stem cells. Following culture, the cells were stained to visualize lipid droplets and calcium deposition (**Figure 5A** and **Figure 6 A**). ImageJ was used to evaluate the percentage area of differentiated cells.

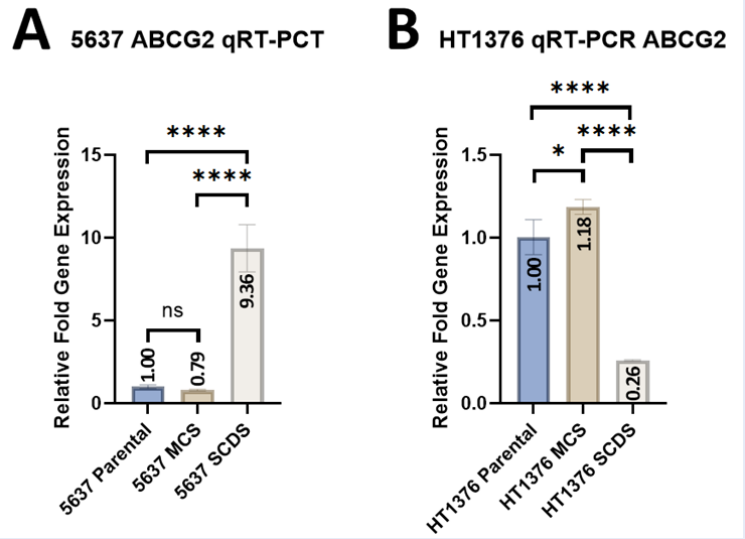

Figure 7: **qRT-PCR analysis of 5637 and HT-1376 Parental, MCS and SCDS ABCG2 drug resistant gene expression**. (**A**) Bar chart of 5637 Parental, MCS and SCDS relative fold gene expression of *ABCG2* drug resistant gene by qRT-PCR. (**B**) Bar chart of HT-1376 Parental, MCS and SCDS relative fold gene expression of ABCG2 drug resistant gene by qRT-PCR. The bars are represented as mean +SD (n = 3). Statistical significance was measured with the two-way ANOVA. *p < 0.05, **p < 0.005, ***p < 0.0005, ****p < 0.0001, ns = not significant. **Abbreviations**: **MCS**: Multicellular Spheroid, **SCDS**: Single Cell-Derived Spheroid

In adipogenic differentiation, 5637 MCS and SCDS showed a lower percentage of differentiation (5.97% ± 1.93 and 5.36% ± 0.74, respectively) when compared to the parental monolayer adherent cells (6.01% ± 0.59) ($p > 0.05$). However, HT-1376 MCSs showed a lower percentage of differentiation, 7.52% ± 2.32 ($p > 0.05$), while SCDS were higher, 9.17% ± 4.57 ($p > 0.05$), compared to parental cells (8.17% ± 3.15 (**Figure 5 B** and **C**)).

In osteogenic differentiation, the MCSs and SCDSs of both 5637 and HT-1376 cells showed a higher percentage of differentiation (26.09% + 5.70, 21.74% + 4.64, 50.11% + 12.80, and 41.04% + 13.43, respectively) than the parental cells (19.80% + 2.62 and 36.13% + 8.84, respectively) ($p > 0.05$) (**Figure 6 B** and **C**).

ABCG2 drug resistance gene expression in the MCS and SCDS of 5637 and HT-1376 cells

To analyze the drug resistance capability of the MCS and SCDS of both 5637 and HT-1376 cells at the molecular level, the gene expression of ABCG2 was analyzed using quantitative qRT–PCR, and the relative expression of genes in MCS and SCDS of both cell lines was compared to the expression of genes in parental monolayer adherent cells of each cell line.

In the 5637 cell line, MCS cells showed lower expression (0.79-fold change) of ABCG2 than 5637 parental monolayer adherent cells ($p > 0.05$), whereas in 5637 SCDS cells, the expression of the ABCG2 drug efflux gene was significantly higher (9.36-fold change) than that in 5637 MCS (0.79-fold change) and parental monolayer adherent cells ($p < 0.0001$) (**Figure 7 A**).

In the HT-1376 cell line, MCS showed upregulation (1.18-fold change) of ABCG2 gene expression when compared with the HT-1376 parental monolayer adherent cells ($p < 0.05$) and SCDS ($p < 0.0001$), as SCDS showed downregulation (0.26-fold change) of ABCG2 drug efflux gene expression when compared with both parental monolayer adherent cells and MCS (1.18-fold change) ($p < 0.0001$) (**Figure 7 B**).

Cell viability assay and cisplatin inhibitory concentration 50 (IC_{50})

To assess the cell viability and IC_{50} of cisplatin for 5637 and HT-1376 cell lines, the parental cells of both cell lines were treated with cisplatin for 48 and 72 hours, respectively.

The IC_{50} values for the 5637 cell line were 1.1 μM for 48 hours of cisplatin treatment and 3.95 μM for 72 hours of cisplatin treatment (**Figure 8 A**). For the HT-1376 cell line, the IC_{50} values for 48 hours and 72 hours of cisplatin treatment were 2.75 μM and 7 μM, respectively (**Figure 8 B**).

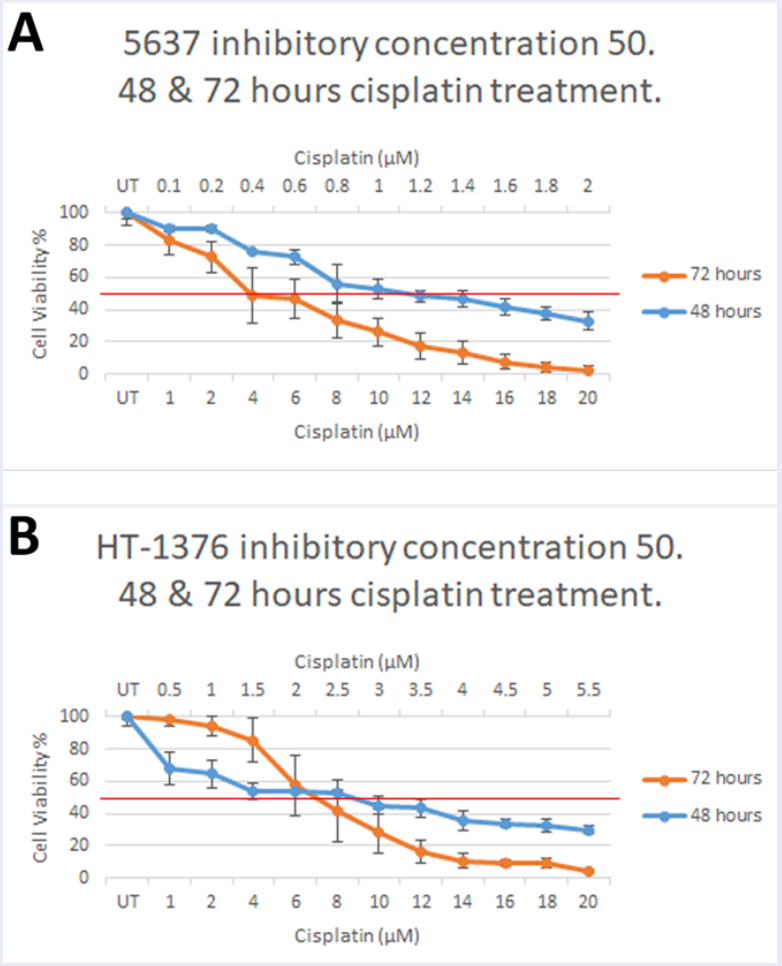

Figure 8: **Cell viability assay and cisplatin inhibitory concentration 50 (IC_{50}) of 5637 and HT-1376 parental cells**. (**A**) Line chart of 5637 parental cell line after 48 and 72 hours of cisplatin treatment. (**B**) Line chart of HT-1376 parental cell line after 48 and 72 hours of cisplatin treatment. **Abbreviations**: **IC50**: Inhibitory Concentration 50%

Spheroid chemotherapy resistance assay

The chemotherapy resistance capability of MCS and SCDS of both 5637 and HT-1376 was evaluated by treating the spheroid with the IC_{50} dose of cisplatin for 48 hours.

In the 5637 cell line, MCS showed a 13.52% reduction in spheroid diameter from 126.96 μm $\pm$ 46.88 to 109.79 μm $\pm$ 40.60 ($p > 0.05$), while in SCDS, there was a 28.36% increase in spheroid diameter post cisplatin treatment, from 113.28 μm $\pm$ 29.52 to 158.11 μm $\pm$ 41.12 ($p < 0.0001$) (**Figure 9 B**).

In the HT-1376 cell line, MCS showed an 18.62% reduction in mean spheroid diameter from 205.64 μm $\pm$ 85.19 to 167.35 μm $\pm$ 55.32 ($p < 0.05$), whereas in SCDS, there was a trend of a small increase (0.2%) in mean spheroid diameter after cisplatin treatment, from 128.77 μm $\pm$ 34.64 to 129.05 μm $\pm$ 34.74 ($p > 0.05$), but the changes were not significant (**Figure 9 B**).

DISCUSSION

Stem cells possess remarkable characteristics, including their ability to undergo self-renewal, generate daughter cells while preserving their stemness, and differentiate into various cell lineages and revert back to a stem-like state through dedifferentiation[41]. These cells play a vital role in the development and maintenance of organs and tissues, contributing to growth and facilitating tissue repair following injury. Similarly, in the context of cancer,

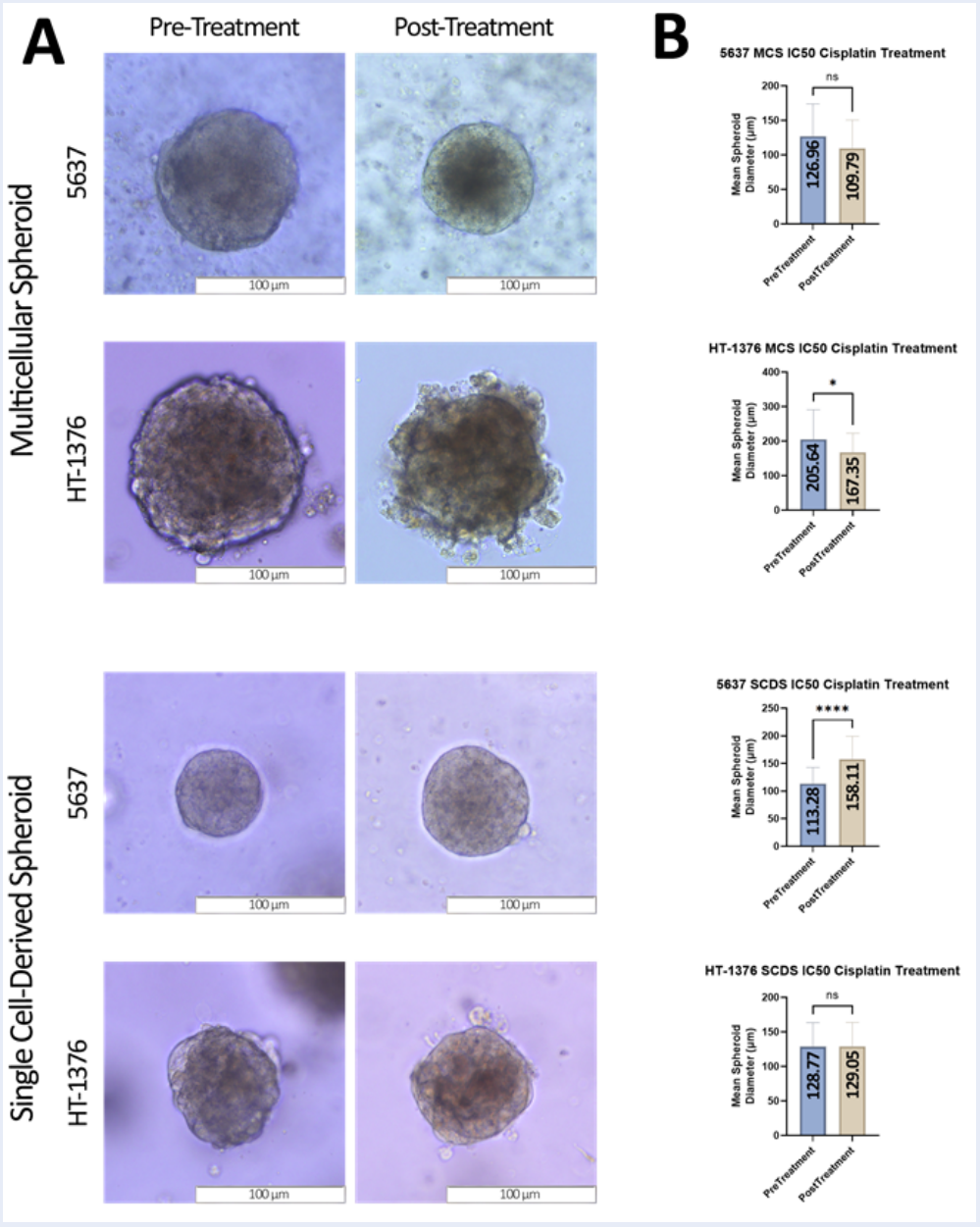

Figure 9: **IC_{50} Cisplatin treatment on MCS and SCDS of 5637 and HT-1376**. (**A**) Culture image of MCS and SCDS of 5637 and HT-1376 pre-treatment and post-treatment with IC_{50} dose of cisplatin, taken at x10 magnification. (**B**) Bar chart of mean spheroid diameter (μm) of MCS and SCDS for 5637 and HT-1376 pre-treatment and post-treatment with IC_{50} dose of cisplatin. The bars are represented as mean +SD (n = 3). Statistical significance was measured with the t-test. *p < 0.05, **p < 0.005, ***p < 0.0005, ****p < 0.0001, ns = not significant. **Abbreviations**: **IC_{50}**: Inhibitory Concentration 50%, **MCS**: MulticellularSpheroid, **SCDS**: SingleCell-Derived Spheroid

there exists a population of cells known as cancer stem cells or tumor-initiating cells, which are responsible for sustaining tumor survival and facilitating recovery. In essence, the tumor itself can be viewed as an independent organ or tissue, regardless of its origin[42]. This concept of stem-like cells within a tumor raises the possibility that cancer may arise not only from clonal evolution resulting from mutations but also from a single cell possessing unlimited self-renewal capability and plasticity. In their quest for survival and proliferation, these stem-like cells employ various mechanisms. For instance, they undergo epithelial-mesenchymal transition (EMT) to facilitate metastasis to neighboring tissues or organs. They also exhibit tumorigenicity, contributing to the reformation of the tumor bulk. Additionally, they develop drug resistance through mechanisms such as entering a quiescent state, repairing DNA damage to avoid apoptosis, or employing drug efflux pumps such as the ATP-binding cassette (ABC) transporter P-glycoprotein. These mechanisms are regulated by feedback control systems involving interactions with neighboring cells in the tumor bulk (paracrine signaling) or self-stimulation (autocrine signaling). These interactions subsequently promote the expansion of stem-like cell populations through asymmetrical cellular division. Based on this hypothesis, the enrichment of stem-like cells or CSCs may be achievable through the generation of three-dimensional (3D) cell structures, such as spheroids.

In this investigation, we successfully generated 3D spheroids using two different approaches. The first approach involved aggregating multiple cells to mimic the aggregation and structure observed *in vivo*. The second approach focused on deriving spheroids from single cancer stem cells and progenitor cells, capitalizing on their self-renewal capabilities. To ensure the optimal growth and survival of the spheroids, we conducted experiments comparing different supplements and various concentrations of FBS. Based on our results (not shown), we determined that a combination of 1% B27 supplement, 20 ng/ml basic fibroblast growth factor (bFGF), 20 ng/ml EGF, and 4 μg/ml insulin was the minimal supplementation required for the growth and viability of our spheroids. Following the culture period with the aforementioned supplement, both the 5637 and HT-1376 cell lines successfully formed spheroids displaying distinct morphological structures. The 5637 spheroids appeared as grape-like clusters of cells with medium to lose cell-to-cell adhesion. In contrast, the HT-1376 spheroids formed compact masses of cells with tight cell-to-cell adhesion. These observations are consistent with previous studies[43,44].

The morphology of the formed spheroids, whether characterized by loose aggregation or a tightly clustered sphere, is determined by the cells' ability to produce specific proteins involved in cell adhesion, such as tight junction protein ZO-1 and cellular adhesion protein E-cadherin[45,46]. These proteins play significant roles in EMT, cell migration, and invasion, as the loss of ZO-1 and E-cadherin is associated with increased EMT and invasiveness, particularly in higher-grade tumors[47–49]. Similar findings have been observed in bladder cancer, where reduced levels of E-cadherin are found in higher-grade and highly metastatic bladder cancers, while higher levels are detected in low-grade bladder cancer and normal urothelial tissue[50–52]. Our results indicate that the grape-like cluster morphology observed in the 5637 spheroids, characterized by loose aggregation, could suggest a lower expression of ZO-1 and E-cadherin compared to the HT-1376 spheroids, which formed tightly clustered masses with strong cell–cell adhesion. It is worth noting that the 5637 cell line originates from grade 2 carcinoma, while the HT-1376 cell line originates from grade 3 carcinoma. The 5637 cells exhibit less differentiation and possess a basal cell morphology, whereas the HT-1376 cells are predominantly differentiated and resemble an umbrella cell morphology. This distinction may explain the stronger cell–cell adhesion observed in the HT-1376 spheroids compared to the 5637 spheroids.

Enrichment of CSCs from cancer cell lines was successfully achieved by either multicellular tumor spheroid formation[10,31,53] or single-cell-derived tumor spheroids[11,31,54–56] in various solid tumors. To study the stemness and enrichment of stem-like cells in both cell lines, we analyzed the pluripotent transcription factors *SOX2*, *NANOG*, and *POU5F1* in cells derived from the MCSs and SCDSs. These pluripotent transcription factors are also known to contribute to somatic cell reprogramming into an ESC-like state, called induced pluripotent stem cells[57,58]. Pluripotent transcription factors are important in sustaining a pluripotency state, with all 3 markers interacting and regulating one another, and are controlled by the MAPK/Wnt signaling pathway and repressed by the SMAD signaling pathway[58]. The downregulation of one of these markers results in a causal determination of the end lineage of the cell, either mesodermal (ME) or neuroectodermal. In the neuroectodermal lineage, overexpression of *SOX2* is maintained, with repression of the *POU5F1* gene, while in the mesodermal lineage, the opposite expression can be seen, with overexpression of *POU5F1* and repression of *SOX2*[58].

Signals to induce differentiation in stem cells are mediated by multiple regulatory mechanisms. Osteogenic differentiation, for example, is mediated by several pathways, such as the Wnt/β-catenin, TGF-β, FGF, Hedgehog, and Notch pathways, while in adipogenic differentiation, the IGF-1, MAPK, glucocorticoid, cAMP and BMP signaling pathways promote adipogenesis. The three key transcription factors *POU5F1, NANOG,* and *SOX2* serve as differentiation repressors in the aforementioned signaling pathways[59–62]. Considering the important role of these transcription factors in stemness, MCS and SCDS were analyzed for the expression of these genes. Unsurprisingly, upregulation of all 3 genes, *POU5F1*, *NANOG* and *SOX2*, was detected in qRT–PCR analysis of MCS and SCDS of both cell lines compared with parental monolayer adherent cells of the respective cell lines. However, the qRT–PCR obtained contradicted the study performed by Ferreira-Teixeira *et al.*, 2015[43], where their HT-1376 spheroid only showed upregulation of *SOX2* gene expression and no changes toward the expression level of *POU5F1* & *NANOG* when compared to parental cells. The result from Ferreira-Teixeira *et al*., 2015[43], is also in disagreement with the result obtained by Atlasi *et al*., 2007[63], where they observed a high level of *POU5F1* in bladder cancer. Amini *et al*., 2014[64], observed an upregulation in the expression of all 3 pluripotent genes, *POU5F1*, *NANOG* and *SOX2,* in bladder cancer cell lines, similar to our results.

The results obtained demonstrate a relative enrichment of CSCs in both spheroid culture methods employed for both cell lines when comparing them to the parental monolayer adherent cells. It is important to note that while the fold change of pluripotent genes was substantially higher in HT-1376 MCS and SCDS compared to 5637 MCS and SCDS, this does not imply a higher enrichment of CSCs in the HT-1376 cell line relative to the 5637 cell line. The fold change serves as a relative comparison to the respective parental monolayer adherent cells, rather than a direct quantitative measurement of the pluripotent transcription factors.

Potency refers to the capability of the cell to give rise and differentiate into a specialized cell lineage[41]. Pluripotent cells are able to transform into various types of adult cells when maintained in the presence of various growth factors[65]. Unlike embryonic stem cells that are totipotent or pluripotent, adult stem cells and cancer stem cells are multipotent and only able to give rise to a limited adult cell lineage that falls in the same germ layer category to which they belong. To prove the existence of bladder cancer stem cells and whether enrichment of the cancer stem cells was achieved, differentiation into adipogenic and osteogenic lineages was performed, as these cell lineages belong to the same mesodermal germ layer as the urinary bladder epithelial cells. Following the differentiation culture assay, both 5637 and HT-1376 parental, MCS and SCDS cells showed differentiation capabilities for both lineages; however, 5637 MCS, 5637 SCDS, and HT-1376 MCS cells showed lower adipogenic differentiation ($p > 0.05$) than the respective parental cells, and only HT-1376 SCDS cells showed higher adipogenic differentiation ($p < 0.05$) than the parental HT1376 cell line. In osteogenic differentiation, the MCS and SCDS of both 5637 and HT-1376 cells showed higher differentiation ($p > 0.05$) when compared to the respective parental cell lines. This shows that the presence of stem-like cells as differentiation into both lineages was successfully achieved.

In bladder cancer, CSCs arise from the basal layer of the epithelium, and studies on bladder cancer stem cells, either isolated or enriched, are often postulated by the presence of basal cell surface markers. Surface markers such as CD24, CD44, CD49f, CD133 and KRT14 are often used as cancer stem cell markers, as these are also markers for bladder urothelium basal cells. While the expression and upregulation of one marker might not be a strong consideration to conclude the presence of CSCs, as these markers are not cancer stem cell exclusive, and there is no consensus on the "best markers" or "specific markers" for CSCs, coexpression and coupregulation of these markers could narrow down the percentage of the true cancer stem cell population. Our findings highlight an increase in the coexpression of CD24 and CD44, CD44 and CD133, and CD133 and CD24 in our entire spheroid samples, indicating a higher number of CSCs due to enrichment of the cell population in both MCSs and SCDSs when compared with cells grown in monolayer culture. This showed that when cells were cultured in the 3D culture method with the addition of growth factors, supplements and minimal serum, the spheroids expressed higher CSC markers, and CSCs were successfully enriched, regardless of whether the spheroid was derived from single cells or formed by forced aggregation of cells.

CD44 is one of the surface markers that has been associated with stem cell characteristics in both normal urothelium and bladder cancer. $CD44^+$ cells are associated with high-grade and high-stage bladder cancer by promoting tumor progression, invasion, metastasis and initiation of epithelial-mesenchymal transition[66–69]. Chan *et al*., 2009[70], found that the $CD44^+$

subpopulation of cells has up to 200 times higher tumorigenicity than the $CD44^-$ subpopulation when transplanted into nude mice. $CD44^+$ samples were also associated with the worst prognosis in patients with low survival and a high recurrence rate[68].

CD24 is also a surface marker that has been used as a stemness marker in various cancers. CD24 works by binding to P-selectin, an adhesion receptor on activated endothelial cells and platelets, indicating that the protein actually increases the ability of cancer cells to metastasize throughout the body[71–73]. In bladder cancer, Ooki *et al.*, 2018[74] associated the presence of $CD24^+$ cells with CSCs, as they observed a reduction in stem cell traits such as sphere-forming capability, self-renewal capability, invasiveness, anti-apoptotic ability and *in vivo* tumorigenicity following knockdown of CD24.

Another surface marker, CD133, appears to be linked to the epithelial-mesenchymal transition and the WNT signaling pathway, implicating it directly in cell proliferation[75]. CD133 has also been found to correlate with hypoxic conditions, where it will play a reciprocal role in preventing hypoxia in tumors by promoting angiogenesis, cell proliferation and cell migration[76]. In bladder cancer, the expression of CD133 was highly expressed in higher grade, metastatic and aggressive tumor behavior[77,78]. Huang *et al.*, 2013[79] observed higher tumorigenicity and cisplatin and BCG resistance in the $CD133^+$ subpopulation of J82 cells than in the $CD133^-$ subpopulation.

The enrichment of the CSC population was confirmed by the upregulation of CSC surface markers and pluripotent transcription gene expression in both MCS and SCDS cultures of the 5637 and HT-1376 cell lines. However, it is essential to investigate whether CSC enrichment correlates with other CSC characteristics, such as drug resistance, and whether CSC enrichment leads to the development of chemotherapy-resistant tumor bulk. Regarding drug resistance, only the 5637 SCDS cells exhibited a significant increase in cisplatin resistance and upregulation of ABCG2, a drug efflux gene. In the spheroid chemotherapy resistance assay, where spheroids were treated with the IC_{50} dose of cisplatin, the 5637 MCS, HT-1376 MCS, and HT-1376 SCDS showed either a decrease in spheroid diameter or no significant change following treatment. However, the 5637 SCDS displayed significant resistance to cisplatin treatment, as evidenced by an increase in spheroid diameter even after drug exposure. It is important to note that the expression of ABCG2 can be dependent on the specific cell line and clonal variation, as not all cells within the same cell line express the ABCG2 gene and protein. This is evident in the 5637 cell line, where the 5637 SCDS, derived from a single cell with self-renewal capability, may express the ABCG2 gene, resulting in progeny with similar gene expression. In contrast, the 5637 MCSs, formed by the forced aggregation of multiple cells to generate spheroids, showed no significant change in ABCG2 gene expression. This difference may be attributed to the cells originating from various clones, with some expressing the ABCG2 gene and others lacking its expression. Therefore, while both the MCS and SCDS methods effectively enriched the CSC population in the 5637 and HT-1376 cell lines, the observed drug resistance and ABCG2 expression were specific to the 5637 SCDS cells. The presence of ABCG2 expression may be influenced by cell line and clonal factors, with single cell-derived spheroids potentially containing cells expressing the ABCG2 gene. The formation of a tumor bulk in the 5637 MCSs resulted in a slower cell proliferation rate. Consequently, the proliferation of cells expressing the ABCG2 gene was also lower than that of 5637 SCDS cells. In the case of 5637 SCDS, the tumor bulk originated from a single cell, allowing for a higher cell proliferation rate during the logarithmic phase of spheroid growth. This also led to a higher proliferation of cells expressing the ABCG2 gene. This difference is evident when examining the growth of spheroid diameter from day 2 to day 10. In the 5637 MCSs, the diameter growth was less significant than that in the 5637 SCDS when comparing the growth from one time point to the next. It is worth noting that the observed increase in spheroid diameter in the 5637 MCSs could be attributed to the aggregation of adjacent cells and spheroids in the culture. In HT-1376 MCS, although there was an increase in ABCG2 gene expression, the spheroid diameter exhibited a reduction when treated with the IC_{50} dose of cisplatin. This observation may be attributed to the fact that the outer layer of the spheroid predominantly consists of cells that do not possess cancer stem cell (CSC) traits, such as drug resistance. Furthermore, the slower growth rate of cells in HT-1376 MCSs, as evidenced by spheroid growth from day 2 to day 10, could contribute to the decrease in spheroid diameter after cisplatin treatment.

CONCLUSIONS

Both the SCDS and MCS methods employed in this study have distinct principles for spheroid development. SCDS relies on the self-renewal capability

of cells to grow in a 3D environment from a single cell, while MCS is based on the cellular organization to mimic the structure of an *in vivo* tumor. Both methods successfully enriched the population of CSCs based on spheroid formation, enrichment of CSC surface markers, pluripotent gene expression, and differentiation potential of cells derived from the spheroids. Comparing the two methods, SCDS demonstrated several advantages. It yielded a higher number of spheroids per well of culture, and the spheroids showed more uniform sizes since aggregation between spheroids was prevented by using a culture scaffold such as Matrigel^{TM}. Moreover, SCDS resulted in higher expression levels of CSC surface markers and pluripotent genes than the MCS method. However, it is important to note that while 3D culture organization was effective in enriching the CSC population, it does not necessarily reflect the chemoresistant potential of the cells. Other factors also contribute to the overall survivability of the cells.

In conclusion, our study demonstrates that culturing cells in a 3D structure successfully enriched the population of bladder CSCs within a relatively short timeframe. The increased number of cells coexpressing CD24, CD44, and CD133 surface markers associated with bladder CSCs, along with the upregulation of transcription factors involved in stemness maintenance, supports the efficacy of 3D culture in enriching CSC populations. However, it is important to note that there were variations and discrepancies observed in the association between 3D culture, CSCs, and drug resistance. These findings highlight the potential of these techniques for the enrichment of cells expressing CSC markers, which could be instrumental in addressing specific therapeutic objectives. We propose the utilization of these methods for comprehensive studies on CSCs, encompassing phenotypic, genotypic, and personalized therapeutic investigations.

ABBREVIATIONS

3D: Three Dimensional, **ABCB5**: ATP-binding cassette sub-family B member 5, **ABCG2**: ATP-binding cassette super-family G member 2, **AC**: Adenocarcinoma, **ALDH**: Aldehyde Dehydrogenase, **AML**: Acute Myeloid Leukaemia, **Anti-PD-1**: Anti-Programmed Death 1, **Anti-PD-L1**: Anti-Programmed Death-Ligand 1, **APC**: Allophycocyanin, **BC**: Bladder Cancer, **BCG**: Bacillus Calmette-Guerin, **BCL-2**: B-cell lymphoma 2, **bFGF**: Basic Fibroblast Growth Factor, **CD133**: Cluster of Differentiation 133, **CD24**: Cluster of Differentiation 24, **CD44**: Cluster of Differentiation 44, **CDKN2A**: Cyclin-Dependent Kinase Inhibitor 2A, **Cis**: Cisplatin, **cMOAT**: canalicular Multispecific Organic Anion Transporter, **c-Myc**: cellular-Myelocytomatosis, **COX**: Cytochrome C Oxidase, **CSC**: Cancer Stem Cell, **CT**: Computerized Tomography, **DMEM**: Dulbecco's Modified Eagle Medium, **DMSO**: Dimethylsufoxide, **DNA**: Deoxyribonucleic Acid, **EDTA**: Ethylenediaminetetraacetic Acid, **EGF**: Epidermal Growth Factor, **EMT**: Epithelial-Mesenchymal Transition, **ERBB2**: Erb-B2 Receptor Tyrosine Kinase 2, **ERBB3**: Erb-B2 Receptor Tyrosine Kinase 3, **ERCC1**: Excision Repair Cross Complementation Group 1, **FACS**: Fluorescence Activated Cell Sorting, **FBS**: Fetal Bovine Serum, **FGFR3**: Fibroblast Growth Factor Receptor 3, **FITC**: Fluorescein Isothiocyanate, **FOXA1**: Forkhead box protein A1, **GAPDH**: Glyceraldehyde 3-Phosphate Dehydrogenase, **GATA3**: GATA Binding Protein 3, **GC**: Gemcitabine and Cisplatin, **Gem**: Gemcitabine, **H3K27**: Histone H3 Lysine 27, **H3K4**: Histone H3 Lysine 4, **hCtr1**: High Affinity Copper Transporter Protein 1, **Her2**: Human Epidermal Growth Factor Receptor 2, **Hh**: Hedgehog, **HIF-1**: Hypoxia-Inducible Factor-1, **HIF-1α**: Hypoxia-Inducible Factor 1-Alpha, **HRAS**: GTPase Hras, **IC**: Inhibitory Concentration, **IGF-1**: Insulin-Like Growth Factor 1, **IGF-2**: Insulin-Like Growth Factor 2, **IL**: Interleukin, **Klf4**: Krueppel-Like Factor 4, **KRT14**: Keratin 14, **KRT20**: Keratin 20, **KRT5**: Keratin 5, **KRT6**: Keratin 6, **MACS**: Magnetic Activated Cell Sorting, **MCS**: Multicellular Spheroid, **MCTS**: Multicellular Tumour Spheroid, **MDR1**: Multidrug Resistance 1, **MET**: Mesenchymal-Epithelial Transition, **MIBC**: Muscle Invasive Bladder Carcinoma, **MRI**: Magnetic Resonance Imaging, **MRP2**: Multispecific Organic Anion Transporter 2, **MTT**: 2,5-Diphenyl-2H-Tetrazolium Bromide, **MVAC**: Methotrexate, Vinblastine, Adriamycin, And Cisplatin, **NAC**: Neoadjuvant Chemotherapy, **NANOG**: Nanog homeobox, **NER**: Nucleotide Excision Repair, **NIHGC**: Noninvasive Papillary HG Urothelial Carcinoma, **NILGC**: Noninvasive Papillary LG Urothelial Carcinoma, **NMIBC**: Non-Muscle Invasive Bladder Carcinoma, **Non-TCC**: Non-Transitional Cell Carcinoma, **NOS**: Nitric Oxide Synthase, **Notch**: Neurogenic Locus Notch Homolog, **OCT4**: Octamer-Binding Transcription Factor 4, **PBS**: Phosphate Buffer Saline, **PDGF-BB**: Platelet-Derived Growth Factor BB, **PDK1**: Pyruvate Dehydrogenase Kinase 1, **PE**: Phycoerythrin, Penstrep: Penicillin-Streptomycin, **PlGF**: Placental Growth Factor, **POU5F1**: POU Class 5 Homeobox 1, **PPARG**: Peroxisome Proliferator Activated Receptor

Gamma, **PUNLMP**: Papillary Urothelial Neoplasm Of Low Malignant Potential, **RB1**: Retinoblastoma 1, **RC**: Radical Cystectomy, **RNA**: Ribonucleic Acid, **ROS**: Reactive Oxygen Species, **RPM**: Revolutions Per Minute, **RPMI-1640**: Rosewell Park Memorial Institute 1640, **SCC**: Squamous Cell Carcinoma, **SCDS**: Single Cell-Derived Spheroid, **SCID**: Severe Combined Immune-Deficient, **SOX2**: SRY (Sex Determining Region Y)-Box 2, **SP**: Side Population, **TCA**: Tricarboxylic Cycle, **TCC**: Transitional Cell Carcinoma, **TERT**: Telomerase Reverse Transcriptase, **TGF**: Transforming Growth Factor, **TNF**: Tumor Necrosis Factor, **TP53**: Tumor Protein 53, **TURBT**: Trans-Urethral Resection Of Bladder Tumor, **UC**: Urothelial Carcinoma, **Ucs**: Undifferentiated Carcinomas, **UV**: Ultraviolet, **VEGF**: Vascular Endothelial Growth Factor, **WHO**: World Health Organization, **Wnt**: Wingless and Int-1, **XPC**: Xeroderma Pigmentosum Complementation Group C.

ACKNOWLEDGMENTS

The authors express their gratitude to the staff and students at Advanced Medical and Dental Institute (IPPT), Universiti Sains Malaysia, Penang, for their invaluable assistance and support provided to Mr. Omar during his research activities and stay.

AUTHOR'S CONTRIBUTIONS

All authors equally contributed to this work. All authors read and approved the final manuscript.

FUNDING

This study was funded by Ministry of Higher Education Malaysia through Fundamental Research Grant Scheme FRGS/1/2019/SKK15/UITM/03/1, Project ID 15531, RMC file number 600- IRMI/FRGS 5/3 (286/2019).

AVAILABILITY OF DATA AND MATERIALS

Data and materials used and/or analyzed during the current study are available from the corresponding author on reasonable request.

ETHICS APPROVAL AND CONSENT TO PARTICIPATE

Not applicable.

CONSENT FOR PUBLICATION

Not applicable.

COMPETING INTERESTS

The authors declare that they have no competing interests.

REFERENCES

1. Bryan RT. Bladder cancer and cancer stem cells: basic science and implications for therapy. TheScientificWorldJournal. 2011;11:1187–94. PMID: 21666988. Available from: https://doi.org/10.1100/tsw.2011.117.
2. Li KLY, Yang Z, Han N, Quan X, Guo X, Li C. Bladder cancer stem cells: clonal origin and therapeutic perspectives. Oncotarget. 2017;8(39):66668–79. PMID: 29029546. Available from: https://doi.org/10.18632/oncotarget.19112.
3. Tang C, Ma J, Liu X, Liu Z. Development and validation of a novel stem cell subtype for bladder cancer based on stem genomic profiling. Stem Cell Research & Therapy. 2020;11(1):457. PMID: 33115513. Available from: https://doi.org/10.1186/s13287-020-01973-4.
4. Yu Z, Pestell TG, Lisanti MP, Pestell RG. Cancer stem cells. The International Journal of Biochemistry & Cell Biology. 2012;44(12):2144–51. PMID: 22981632. Available from: https://doi.org/10.1016/j.biocel.2012.08.022.
5. Zhang Y, Zhang X, Huang X, Tang X, Zhang M, Li Z, et al. Tumor stemness score to estimate epithelial-to-mesenchymal transition (EMT) and cancer stem cells (CSCs) characterization and to predict the prognosis and immunotherapy response in bladder urothelial carcinoma. Stem Cell Research & Therapy. 2023;14(1):15. PMID: 36721217. Available from: https://doi.org/10.1186/s13287-023-03239-1.
6. Marc F. Botteman CLP, Alberto Redaelli, Benjamin Laskin, Robert Hauser. The Health Economics of Bladder Cancer. PharmacoEconomics. 2003;21:1315–30. PMID: 14750899. Available from: https://doi.org/10.1007/BF03262330.
7. Tan J, Wang Y, Sun L, Xu S, Li C, Jin X. The Origin and Evolution of Bladder Cancer Stem Cells. Frontiers in Cell and Developmental Biology. 2022;10:950241. PMID: 35903544. Available from: https://doi.org/10.3389/fcell.2022.950241.
8. Lander AD. The 'stem cell' concept: is it holding us back? Journal of Biology. 2009;8(8):70. PMID: 19769787. Available from: https://doi.org/10.1186/jbiol177.
9. Plaks V, Kong N, Werb Z. The cancer stem cell niche: how essential is the niche in regulating stemness of tumor cells? Cell Stem Cell. 2015;16(3):225–38. PMID: 25748930. Available from: https://doi.org/10.1016/j.stem.2015.02.015.
10. Herheliuk T, Perepelytsina O, Ugnivenko A, Ostapchenko L, Sydorenko M. Investigation of multicellular tumor spheroids enriched for a cancer stem cell phenotype. Stem Cell Investigation. 2019;6:21. PMID: 31559308. Available from: https://doi.org/10.21037/sci.2019.06.07.
11. Lapidot T, Sirard C, Vormoor J, Murdoch B, Hoang T, Caceres-Cortes J, et al. A cell initiating human acute myeloid leukaemia after transplantation into SCID mice. Nature. 1994;367(6464):645–8. Available from: https://doi.org/10.1038/367645a0.
12. Al-Hajj M, Clarke MF. Self-renewal and solid tumor stem cells. Oncogene. 2004;23(43):7274–82. PMID: 15378087. Available from: https://doi.org/10.1038/sj.onc.1207947.
13. Sheila K. Singh IDC, Mizuhiko Terasaki, Victoria E. Bonn, Cynthia Hawkins, Jeremy Squire, Peter B. Dirks. Identification of a Cancer Stem Cell in Human Brain Tumors. Cancer Research. 2003;63:5821–8.
14. Fang D, Nguyen TK, Leishear K, Finko R, Kulp AN, Hotz S. A tumorigenic subpopulation with stem cell properties in melanomas. Cancer Research. 2005;65(20):9328–37. PMID: 16230395. Available from: https://doi.org/10.1158/0008-5472.CAN-05-1343.
15. Tirino V, Desiderio V, d'Aquino R, Francesco FD, Pirozzi G, Graziano A. Detection and characterization of CD133+ cancer stem cells in human solid tumours. PLoS One. 2008;3(10):e3469. PMID: 18941626. Available from: https://doi.org/10.1371/journal.pone.0003469.

16. Collins AT, Berry PA, Hyde C, Stower MJ, Maitland NJ. Prospective identification of tumorigenic prostate cancer stem cells. Cancer Research. 2005;65(23):10946–51. PMID: 16322242. Available from: https://doi.org/10.1158/0008-5472.CAN-05-2018.
17. Sharmila A. bapat AMM, Chaitanyananda B. Koppikar, Nawneet K. Kurrey. Stem and Progenitor-Like Cells Contribute to the Aggresive Behavior of Human Epithelial Ovarian Cancer. Cancer Research. 2005;65(8):3025–9. PMID: 15833827. Available from: https://doi.org/10.1158/0008-5472.CAN-04-3931.
18. Takaishi S, Okumura T, Tu S, Wang SS, Shibata W, Vigneshwaran R. Identification of gastric cancer stem cells using the cell surface marker CD44. Stem Cells (Dayton, Ohio). 2009;27(5):1006–20. PMID: 19415765. Available from: https://doi.org/10.1002/stem.30.
19. Eramo A, Lotti F, Sette G, Pilozzi E, Biffoni M, Virgilio AD. Identification and expansion of the tumorigenic lung cancer stem cell population. Cell Death and Differentiation. 2008;15(3):504–14. PMID: 18049477. Available from: https://doi.org/10.1038/sj.cdd.4402283.
20. Tirino V, Camerlingo R, Franco R, Malanga D, Rocca AL, Viglietto G. The role of CD133 in the identification and characterisation of tumour-initiating cells in non-small-cell lung cancer. European Journal of Cardio-Thoracic Surgery. 2009;36(3):446–53. PMID: 19464919. Available from: https://doi.org/10.1016/j.ejcts.2009.03.063.
21. Zakaria N, Yusoff NM, Zakaria Z, Lim MN, Baharuddin PJ, Fakiruddin KS. Human non-small cell lung cancer expresses putative cancer stem cell markers and exhibits the transcriptomic profile of multipotent cells. BMC Cancer. 2015;15(1):84. PMID: 25881239. Available from: https://doi.org/10.1186/s12885-015-1086-3.
22. jie Duan WQJ, Sen-lin X, Bin W, Xian-zong Y, Yi-fang P, Xia Z, et al. Strategies for Isolating and Enriching Cancer Stem Cells: Well Begun Is Half Done. Stem Cells and Development. 2013;22:2221–39. PMID: 23540661. Available from: https://doi.org/10.1089/scd.2012.0613.
23. Saltanatpour Z, Johari B, Alizadeh A, Lotfinia M, Majidzadeh-A K, Nikbin B. Enrichment of cancer stem-like cells by the induction of epithelial-mesenchymal transition using lentiviral vector carrying E-cadherin shRNA in HT29 cell line. Journal of Cellular Physiology. 2019;234(12):22935–46. PMID: 31111504. Available from: https://doi.org/10.1002/jcp.28855.
24. Bertolini G, Roz L, Perego P, Tortoreto M, Fontanella E, Gatti L. Highly tumorigenic lung cancer CD133+ cells display stem-like features and are spared by cisplatin treatment. Proceedings of the National Academy of Sciences of the United States of America. 2009;106(38):16281–6. PMID: 19805294. Available from: https://doi.org/10.1073/pnas.0905653106.
25. Yajima HOT, Uchiyama T, Takano N, Shibahara T, Azuma T. Resistance to cytotoxic chemotherapy-induced apoptosis in side population cells of human oral squamous cell carcinoma cell line Ho-1-N-1. International Journal of Oncology. 2009;35(2):273–80. PMID: 19578740.
26. Wang J, Guo LP, Chen LZ, Zeng YX, Lu SH. Identification of cancer stem cell-like side population cells in human nasopharyngeal carcinoma cell line. Cancer Research. 2007;67(8):3716–24. PMID: 17440084. Available from: https://doi.org/10.1158/0008-5472.CAN-06-4343.
27. Cole JM, Joseph S, Sudhahar CG, Dahl KD. Enrichment for Chemoresistant Ovarian Cancer Stem Cells from Human Cell Lines. Journal of Visualized Experiments. 2014;10(91):e51891. Available from: https://doi.org/10.3791/51891.
28. Abubaker K, Latifi A, Luwor R, Nazaretian S, Zhu H, Quinn MA, et al. Short-term single treatment of chemotherapy results in the enrichment of ovarian cancer stem cell-like cells leading to an increased tumor burden. Molecular Cancer. 2013;12(24):1–15. Available from: https://doi.org/10.1186/1476-4598-12-24.
29. Tang QL, Liang Y, Xie XB, Yin JQ, Zou CY, Zhao ZQ. Enrichment of osteosarcoma stem cells by chemotherapy. Chinese Journal of Cancer. 2011;30(6):426–32. PMID: 21627865. Available from: https://doi.org/10.5732/cjc.011.10127.
30. Wang L, Liu X, Ren Y, Zhang J, Chen J, Zhou W, et al. Cisplatin-enriching cancer stem cells confer multidrug resistance in non-small cell lung cancer via enhancing TRIB1/HDAC activity. Cell Death & Disease. 2017;8(4):e2746. PMID: 28406482. Available from: https://doi.org/10.1038/cddis.2016.409.
31. Lee JW, Sung JS, Park YS, Chung S, Kim YH. Isolation of spheroid-forming single cells from gastric cancer cell lines: enrichment of cancer stem-like cells. BioTechniques. 2018;65(4):197–203. PMID: 30284938. Available from: https://doi.org/10.2144/btn-2018-0046.
32. Zhang S, Sun Y, Sui Y, Li Y, Luo Z, Xu X. Determining Osteogenic Differentiation Efficacy of Pluripotent Stem Cells by Telomerase Activity. Tissue Engineering and Regenerative Medicine. 2018;15(6):751–60. PMID: 30603593. Available from: https://doi.org/10.1007/s13770-018-0138-6.
33. Yang Z, Li C, Fan Z, Liu H, Zhang X, Cai Z. Single-cell Sequencing Reveals Variants in ARID1A, GPRC5A and MLL2 Driving Self-renewal of Human Bladder Cancer Stem Cells. European Urology. 2017;71(1):8–12. PMID: 27387124. Available from: https://doi.org/10.1016/j.eururo.2016.06.025.
34. Wang X, Pan L, Lu Q, Huang H, Feng C, Tao Y. A combination of ssGSEA and mass cytometry identifies immune microenvironment in muscle-invasive bladder cancer. Journal of Clinical Laboratory Analysis. 2021;35(5):e23754. PMID: 33813769. Available from: https://doi.org/10.1002/jcla.23754.
35. Pastrana E, Silva-Vargas V, Doetsch F. Eyes wide open: a critical review of sphere-formation as an assay for stem cells. Cell Stem Cell. 2011;8(5):486–98. PMID: 21549325. Available from: https://doi.org/10.1016/j.stem.2011.04.007.
36. Weiswald LB, Bellet D, Dangles-Marie V. Spherical cancer models in tumor biology. Neoplasia (New York, NY). 2015;17(1):1–15. PMID: 25622895. Available from: https://doi.org/10.1016/j.neo.2014.12.004.
37. Nath S, Devi GR. Three-dimensional culture systems in cancer research: focus on tumor spheroid model. Pharmacology & Therapeutics. 2016;163:94–108. PMID: 27063403. Available from: https://doi.org/10.1016/j.pharmthera.2016.03.013.
38. Souza AG, Silva IB, Campos-Fernandez E, Barcelos LS, Souza JB, Marangoni K. Comparative Assay of 2D and 3D Cell Culture Models: Proliferation, Gene Expression and Anticancer Drug Response. Current Pharmaceutical Design. 2018;24(15):1689–94. PMID: 29623827. Available from: https://doi.org/10.2174/1381612824666180404152304.
39. Jeon S, Lee HS, Lee GY, Park G, Kim TM, Shin J. Shift of EMT gradient in 3D spheroid MSCs for activation of mesenchymal niche function. Scientific Reports. 2017;7(1):6859. PMID: 28761088. Available from: https://doi.org/10.1038/s41598-017-07049-3.
40. Ayob AZ, Ramasamy TS. Cancer stem cells as key drivers of tumour progression. Journal of Biomedical Science. 2018;25(1):20. PMID: 29506506. Available from: https://doi.org/10.1186/s12929-018-0426-4.
41. Singh VK, Saini A, Kalsan M, Kumar N, Chandra R. Describing the Stem Cell Potency: The Various Methods of Functional Assessment and In silico Diagnostics. Frontiers in Cell and Developmental Biology. 2016;4:134. PMID: 27921030. Available from: https://doi.org/10.3389/fcell.2016.00134.
42. Enderling H. Cancer stem cells: small subpopulation or evolving fraction? Integrative Biology. 2015;7(1):14–23. PMID: 25359461. Available from: https://doi.org/10.1039/C4IB00191E.
43. Ferreira-Teixeira M, Parada B, Rodrigues-Santos P, Alves V, Ramalho JS, Caramelo F. Functional and molecular characterization of cancer stem-like cells in bladder cancer: a potential signature for muscle-invasive tumors. Oncotarget. 2015;6(34):36185–201. PMID: 26452033. Available from: https://doi.org/10.18632/oncotarget.5517.
44. Ducci G, Pasquale V, Rota S, Arrigoni E, Campioni G, Ventura E. Profiling Metabolic and Signaling Phenotype of Bladder Cancer Cell Lines. The FASEB Journal. 2022;36. Available from:

https://doi.org/10.1096/fasebj.2022.36.S1.L7639.
45. Edmondson R, Broglie JJ, Adcock AF, Yang L. Three-dimensional cell culture systems and their applications in drug discovery and cell-based biosensors. Assay and Drug Development Technologies. 2014;12(4):207–18. PMID: 24831787. Available from: https://doi.org/10.1089/adt.2014.573.
46. Yoshida T, Sopko NA, Kates M, Liu X, Joice G, Mcconkey DJ. Impact of spheroid culture on molecular and functional characteristics of bladder cancer cell lines. Oncology Letters. 2019;18(5):4923–9. PMID: 31612003. Available from: https://doi.org/10.3892/ol.2019.10786.
47. Martin TA, Jiang WG. Loss of tight junction barrier function and its role in cancer metastasis. Biochimica et Biophysica Acta. 2009;1788(4):872–91. PMID: 19059202. Available from: https://doi.org/10.1016/j.bbamem.2008.11.005.
48. Na TY, Schecterson L, Mendonsa AM, Gumbiner BM. The functional activity of E-cadherin controls tumor cell metastasis at multiple steps. Proceedings of the National Academy of Sciences of the United States of America. 2020;117(11):5931–7. PMID: 32127478. Available from: https://doi.org/10.1073/pnas.1918167117.
49. Lee YC, Tsai KW, Liao JB, Kuo WT, Chang YC, Yang YF. High expression of tight junction protein 1 as a predictive biomarker for bladder cancer grade and staging. Scientific Reports. 2022;12(1):1496. PMID: 35087173. Available from: https://doi.org/10.1038/s41598-022-05631-y.
50. JM MF. Y. Takechi, S. Arakawa, S. Kamidono. The significance of E-cadherin in transitional-cell carcinoma of the human urinary bladder. World Journal of Urology. 1996;14:12–5.
51. Wakatsuki S, Watanabe R, Saito K, Saito T, Katagiri A, Sato S, et al. Loss of human E-cadherin (ECD) correlated with invasiveness of transitional cell cancer in the renal pelvis, ureter and urinary bladder. Cancer Letters. 1996;103(1):11–7. Available from: https://doi.org/10.1016/0304-3835(96)04194-8.
52. Sun W, Herrera GA. E-cadherin expression in invasive urothelial carcinoma. Annals of Diagnostic Pathology. 2004;8(1):17–22. PMID: 15129905. Available from: https://doi.org/10.1016/j.anndiagpath.2003.11.007.
53. Zhong Y, Guan K, Guo S, Zhou C, Wang D, Ma W. Spheres derived from the human SK-RC-42 renal cell carcinoma cell line are enriched in cancer stem cells. Cancer Letters. 2010;299(2):150–60. PMID: 20846785. Available from: https://doi.org/10.1016/j.canlet.2010.08.013.
54. Saadin K, White IM. Breast cancer stem cell enrichment and isolation by mammosphere culture and its potential diagnostic applications. Expert Review of Molecular Diagnostics. 2013;13(1):49–60. PMID: 23256703. Available from: https://doi.org/10.1586/erm.12.117.
55. Liu J, Ma L, Xu J, Liu C, Zhang J, Liu J. Spheroid body-forming cells in the human gastric cancer cell line MKN-45 possess cancer stem cell properties. International Journal of Oncology. 2013;42(2):453–9. PMID: 23229446. Available from: https://doi.org/10.3892/ijo.2012.1720.
56. Chen YC, Ingram PN, Fouladdel S, McDermott SP, Azizi E, Wicha MS. High-Throughput Single-Cell Derived Sphere Formation for Cancer Stem-Like Cell Identification and Analysis. Scientific Reports. 2016;6(1):27301. PMID: 27292795. Available from: https://doi.org/10.1038/srep27301.
57. Okita K, Ichisaka T, Yamanaka S. Generation of germline-competent induced pluripotent stem cells. Nature. 2007;448(7151):313–7. PMID: 17554338. Available from: https://doi.org/10.1038/nature05934.
58. Swain N, Thakur M, Pathak J, Swain B. SOX2, OCT4 and NANOG: the core embryonic stem cell pluripotency regulators in oral carcinogenesis. Journal of Oral and Maxillofacial Pathology : JOMFP. 2020;24(2):368–73. PMID: 33456249. Available from: https://doi.org/10.4103/jomfp.JOMFP_22_20.
59. Huang W, Yang S, Shao J, Li YP. Signaling and transcriptional regulation in osteoblast commitment and differentiation. Frontiers in Bioscience. 2007;12(8-12):3068–92. PMID: 17485283. Available from: https://doi.org/10.2741/2296.
60. Ambele MA, Dhanraj P, Giles R, Pepper MS. Adipogenesis: A Complex Interplay of Multiple Molecular Determinants and Pathways. International Journal of Molecular Sciences. 2020;21(12):4283. PMID: 32560163. Available from: https://doi.org/10.3390/ijms21124283.
61. Zhang K, Yang X, Zhao Q, Li Z, Fu F, Zhang H. Molecular Mechanism of Stem Cell Differentiation into Adipocytes and Adipocyte Differentiation of Malignant Tumor. Stem Cells International. 2020;2020:8892300. PMID: 32849880. Available from: https://doi.org/10.1155/2020/8892300.
62. Thomas S, Jaganathan BG. Signaling network regulating osteogenesis in mesenchymal stem cells. Journal of Cell Communication and Signaling. 2022;16(1):47–61. PMID: 34236594. Available from: https://doi.org/10.1007/s12079-021-00635-1.
63. Atlasi Y, Mowla SJ, Ziaee SA, Bahrami AR. OCT-4, an embryonic stem cell marker, is highly expressed in bladder cancer. International Journal of Cancer. 2007;120(7):1598–602. PMID: 17205510. Available from: https://doi.org/10.1002/ijc.22508.
64. Amini S, Fathi F, Mobalegi J, Sofimajidpour H, Ghadimi T. The expressions of stem cell markers: Oct4, Nanog, Sox2, nucleostemin, Bmi, Zfx, Tcl1, Tbx3, Dppa4, and Esrrb in bladder, colon, and prostate cancer, and certain cancer cell lines. Anatomy & Cell Biology. 2014;47(1):1–11. PMID: 24693477. Available from: https://doi.org/10.5115/acb.2014.47.1.1.
65. Kashyap V, Rezende NC, Scotland KB, Shaffer SM, Persson JL, Gudas LJ. Regulation of stem cell pluripotency and differentiation involves a mutual regulatory circuit of the NANOG, OCT4, and SOX2 pluripotency transcription factors with polycomb repressive complexes and stem cell microRNAs. Stem Cells and Development. 2009;18(7):1093–108. PMID: 19480567. Available from: https://doi.org/10.1089/scd.2009.0113.
66. McKenney JK, Desai S, Cohen C, Amin MB. Discriminatory immunohistochemical staining of urothelial carcinoma in situ and non-neoplastic urothelium: an analysis of cytokeratin 20, p53, and CD44 antigens. The American Journal of Surgical Pathology. 2001;25(8):1074–8. PMID: 11474293. Available from: https://doi.org/10.1097/00000478-200108000-00013.
67. Wu CT, Lin WY, Chen WC, Chen MF. Predictive Value of CD44 in Muscle-Invasive Bladder Cancer and Its Relationship with IL-6 Signaling. Annals of Surgical Oncology. 2018;25(12):3518–26. PMID: 30128900. Available from: https://doi.org/10.1245/s10434-018-6706-0.
68. Siddiqui Z, Srivastava AN, Sankhwar SN, Dalela D, Singh V, Zaidi N. Synergic effects of cancer stem cells markers, CD44 and embryonic stem cell transcription factor Nanog, on bladder cancer prognosis. British Journal of Biomedical Science. 2020;77(2):69–75. PMID: 31718471. Available from: https://doi.org/10.1080/09674845.2019.1692761.
69. Gaiteiro C, Soares J, Relvas-Santos M, Peixoto A, Ferreira D, Paulo P. Glycoproteogenomics characterizes the CD44 splicing code associated with bladder cancer invasion. Theranostics. 2022;12(7):3150–77. PMID: 35547758. Available from: https://doi.org/10.7150/thno.67409.
70. Chan KS, Espinosa I, Chao M, Wong D, Ailles L, Diehn M. Identification, molecular characterization, clinical prognosis, and therapeutic targeting of human bladder tumor-initiating cells. Proceedings of the National Academy of Sciences of the United States of America. 2009;106(33):14016–21. PMID: 19666525. Available from: https://doi.org/10.1073/pnas.0906549106.
71. Hofner T, Macher-Goeppinger S, Klein C, Schillert A, Eisen C, Wagner S. Expression and prognostic significance of cancer stem cell markers CD24 and CD44 in urothelial bladder cancer xenografts and patients undergoing radical cystectomy. Urologic Oncology. 2014;32(5):678–86. PMID: 24631171. Available from: https://doi.org/10.1016/j.urolonc.2014.01.001.
72. Wasfy RE, El-Guindy DM. CD133 and CD44 as cancer stem cell markers in bladder carcinoma. Egyptian Journal of Pathology. 2017;37(1):204–8. Available from: https://doi.org/10.1097/01.

XEJ.0000520912.41715.09.

73. Liu C, Zheng S, Shen H, Xu K, Chen J, Li H. Clinical significance of CD24 as a predictor of bladder cancer recurrence. Oncology Letters. 2013;6(1):96–100. PMID: 23946784. Available from: https://doi.org/10.3892/ol.2013.1357.
74. Ooki A, VandenBussche CJ, Kates M, Hahn NM, Matoso A, McConkey DJ. CD24 regulates cancer stem cell (CSC)-like traits and a panel of CSC-related molecules serves as a non-invasive urinary biomarker for the detection of bladder cancer. British Journal of Cancer. 2018;119(8):961–70. PMID: 30327565. Available from: https://doi.org/10.1038/s41416-018-0291-7.
75. Schmohl JU, Vallera DA. CD133, Selectively Targeting the Root of Cancer. Toxins. 2016;8(6):165. PMID: 27240402. Available from: https://doi.org/10.3390/toxins8060165.
76. Behrooz AB, Syahir A, Ahmad S. CD133: beyond a cancer stem cell biomarker. Journal of Drug Targeting. 2019;27(3):257–69. PMID: 29911902. Available from: https://doi.org/10.1080/1061186X.2018.1479756.
77. Farid RM, Sammour SA, ElDin ZAS, Salman MI, Omran TI. Expression of CD133 and CD24 and their different phenotypes in urinary bladder carcinoma. Cancer Management and Research. 2019;11:4677–90. PMID: 31213893. Available from: https://doi.org/10.2147/CMAR.S198348.
78. Hacek J, Brisuda A, Babjuk M, Zamecnik J. Expression of cancer stem cells markers in urinary bladder urothelial carcinoma and its precursor lesions. Biomedical Papers of the Medical Faculty of the University Palacky, Olomouc, Czechoslovakia. 2021;165(3):316–21. PMID: 32424373. Available from: https://doi.org/10.5507/bp.2020.017.
79. Huang P, Watanabe M, Kaku H, Ueki H, Noguchi H, Sugimoto M. Cancer stem cell-like characteristics of a CD133+ subpopulation in the J82 human bladder cancer cell line. Molecular and Clinical Oncology. 2013;1(1):180–4. PMID: 24649144. Available from: https://doi.org/10.3892/mco.2012.29.